ACADEMY OF AGRICULTURE

"NIKOLA POUSHKAROV" INSTITUTE OF SOIL SCIENCE,
AGROTECHNOLOGIES AND PLANT PROTECTION

BLAGOJ ELENOV

RESEARCH OF SPRAYING COMPONENTS OF AN AIR-ASSISTED SPRAYERS FOR SMALL FARMS

AUTO-REFEREE

of a dissertation for awarding the educational and scientific "PhD degree"

Professional Direction: 5.1. Mechanical Engineering Specialty: "Mechanization and electrification of crop production"

Scientific supervisor: Prof. Dr. Eng.-Math. Georgi Kostadinov

Sofia, 2023

The dissertation work was examined at a meeting of the scientific council at the "Mechanization of agriculture and hydromelioration systems" department at IPAZR "N. Pushkarov", Sofia.

The dissertation student works as an assistant at the "Agricultural Mechanization and Hydromelioration Systems" section at IPAZR "Nikola Pushkarov".

Scientific jury:

1. Prof. Dr. Eng. Snezhan Ivanov Bozhkov – ISSAPP «N. Pushkarov" - chairman
2. Assoc. Dr. Eng. Todor Gergov Penyashki – ISSAPP «N. Pushkarov»
3. Prof. Dr. Eng. Krasimir Mihailov Trendafilov – Stara Zagora Technical University
4. Assoc. Ph.D. Eng. Atanas Zdravkov Atanasov – RU «Angel Kanchev» - Ruse
5. Assoc. Dr. Eng. Manol Angelov Dallev - AU Plovdiv

RELEVANCE OF THE SUBJECT

Chemical plant protection is and will continue to be a major limiting factor in high yield efficient agriculture. This is especially true for permanent plantations, where the costs of plant protection reach up to 40% of the costs required for growing the produce. Plant protection has a multidisciplinary nature. One of the main elements of its implementation is related to the technique used and the possible technological solutions. Knowing the variety of technical solutions and technologies allows to optimize their applicability and operational characteristics according to the specific enemy and culture. In this way, maximum economic and biological efficiency of the event can be achieved. The maximum utilization of the working fluid and minimum pollution of the environment can be achieved by using optimal design and operating parameters of the sprinklers, tailored to the parameters of the sprayed object. A possibility for this is the research and determination of the working parameters of a spraying system of a sprayer for permanent crops intended for small farmers, which allows reaching the maximum biological and economic efficiency of the event in the treatment of permanent crops in conditions of the deepening economic crisis.

SCIENTIFIC NOVELTY

Prerequisites for increasing the effective utilization of pesticide formulations, increasing ecological-economic efficiency and reducing losses have been defined. A coefficient of beneficial use of the pesticide is justified, which allows a quantitative assessment of the use of the pesticide as intended. The graphic interpretation is proposed, which can be used to plan the consumption rate depending on the density, diameter of the drops and plant development recommended for the specific event.

PRACTICAL USEFULNESS

In the present work, technical solutions of air-assisted rotary sprayers have been researched and proposed, and their parameters and modes of operation have been substantiated to achieve the desired droplet coverage, thus creating prerequisites for reducing the costs of carrying out a given plant protection measure and of pollution of the environment and agricultural production.

OBJECT OF THE RESEARCH

The subject of the study is fan rotary diffusers (own design) with varying diameters, diffusers, and blade surface areas.

SUBJECT OF RESEARCH

The subject of the research are the parameters and modes of operation of air-assisted rotary sprayers to an air-assisted sprayer.

Chapter 1. STATE OF THE PROBLEM

In perennial crops in R.Bulgaria, the costs of plant protection operations are the lowest in efficiency compared to other crops and occupy a major share of material costs and mechanized

works. Literature data show that the optimal diameter of the drops is directly related to the operating conditions. In principle, the droplet coating realized by rotary sprayers has a smaller diameter and the drops have a more uniform composition than in the case of hydraulic and pneumatic spraying. In our country, rotary sprayers have not been sufficiently studied, and abroad, the influence of various factors on the drop formation process has not been fully clarified. The high velocities of the laminar air flow, in turn, create a kind of wall that makes it difficult for the sprayer bloom to penetrate inside the vineyard. The parameters of the air flow created by axial fans have also been insufficiently studied.

Chapter 2. OBJECTIVE, TASKS AND RESEARCH METHODOLOGY

OBJECTIVE

Justification of the parameters and operating modes of a fan sprayer for small farming operations.

TASKS

1. Theoretical development of the process of spreading the working liquid from fan sprayers.
2. Justification of the controllable factors and parameters characterizing the mode of operation of rotary nozzles when working with air-assisted sprayers.
3. Development of methodology and stands for conducting experimental studies of the process of spreading and transporting the working fluid to the treated object.
4. Determining the air flow profile for different axial fans.
5. Determining the parameters of the droplet coating in different modes and distance from the spreader.
6. Justification of the optimal mode of operation and arrangement of the fans depending on the type of secret plantations, in order to obtain an even distribution of the working liquid.
7. Justification of the elements of a spraying system for operation on the technology of controlled drop coating.

OBJECT OF THE RESEARCH

The object of the study includes three structural configurations (Fig. 2.1, Fig. 2.2, and Fig. 2.3) of a air-assisted rotary spraying device, as follows:

- Φ500 with a diameter of 500 mm and five trapezoidal-shaped blades with a blade area of 97 cm^2. (fig. 2.1)
- Φ600 M1 with a diameter of 600 mm and seven trapezoidal-shaped blades with a blade area of 161.87 cm^2. (fig. 2.2)
- Φ600 M2 with a diameter of 600 mm and seven rectangular-shaped blades with a blade area of 228 cm^2. (fig. 2.3)

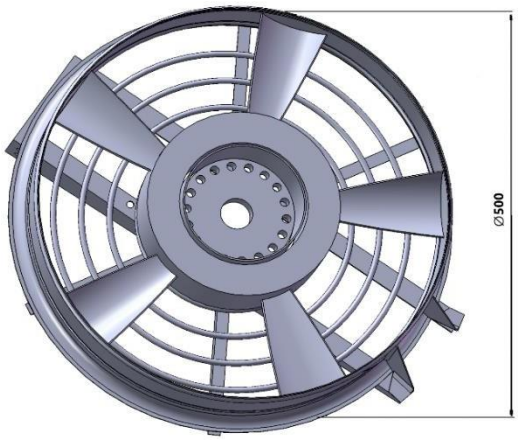
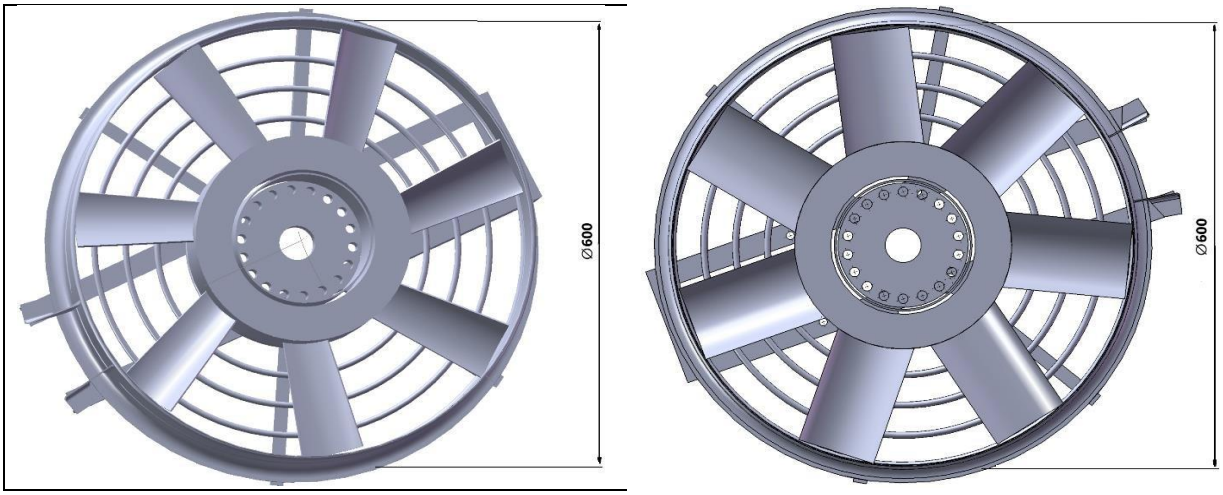


Fig. 2.1. *Fan rotary spreading device with a diameter of Φ500 mm and five fins*



a) b)

Fig 2.2 *Fan rotary spreaders with a diameter of 600 mm with a different blade profile, seven in number*

(a) Modification M1
(b) Modification M2



Fig. 2.3 *General view of a fan-rotary spreading device*

Rotary net type spreader

Conical rotary spreader
Protective grille

Fan
Protective cover

RESEARCH METHODOLOGY OF SPRAYERS OWN CONSTRUCTION

The three modifications of the fan part of the fan rotary air-assisted sprayers developed by us are hydraulically driven. They were tested as connected to a hydraulic station according to the scheme shown in fig. 2.4. From the scheme of the experimental setup, it can be seen that the two working bodies are connected in series, which implies that they have the same frequency of rotation. The technological process proceeds as follows. First, the desired rotation frequency of the spreaders is set. Changing the rotation frequency is achieved by changing the flow rate of the hydraulic oil by means of a flow regulator (6.1). The two fans are driven by hydraulic motors (2). On the hub of the spreader, to which no working fluid is supplied, a reflective patch is stuck and the circular frequency is measured by means of a reflective photoelectric sensor [Salvarani srl] to the measuring device "ALMEMO" (5).

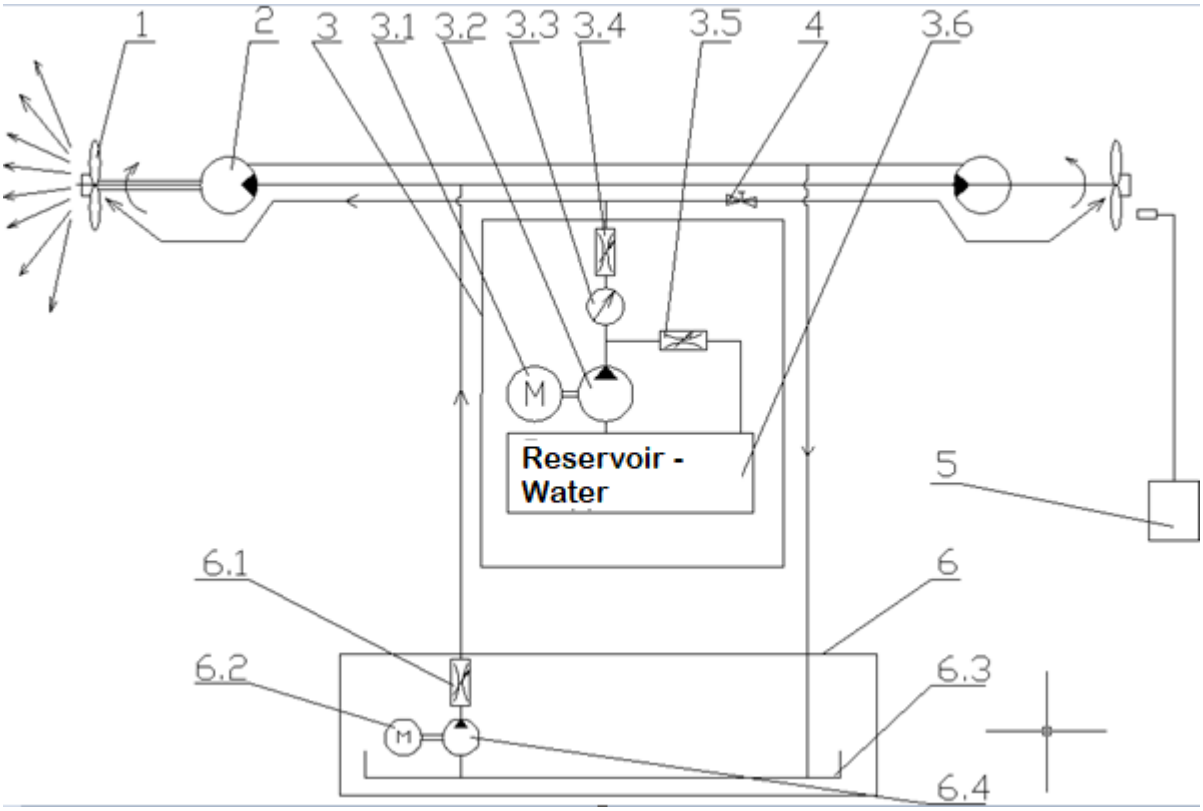


Fig. 2.4. *Schematic of the experimental setup*

1. *Fan; 2. Hydraulic motor; 3. You feed the block with working fluid; 3.1. El. Engine for the pump; 3.2. Pump; 3.3. Manometer; 3.4. Flow regulator; 3.5. Regulator of the stream; 3.6. Water tank; 4. Shut-off valve; 5. Frequency counter; 6. Driving hydro station; 6.1. Flow regulator; 6.2. El. Engine of the hydraulic station; 6.3.Hydraulic oil tank; 6.4. Hydraulic pump.*

RESEARCH OF THE DISTRIBUTION OF THE WORKING FLUID AT THE WORKING HEIGHT OF THE SPRAYER

The study of the distribution of the working fluid is carried out on a bench to establish the vertical distribution. Manufacturer of the device is "Salvarani-II Banco Prova Atomizzatori Verticale" (fig. 2.5.). The device has 20 catch trays, where the working fluid sprayed by the fan rotary sprayers is caught. Each collecting tray is connected by a hose to a numbered test tube, where the captured working fluid is collected. The height of the vertical patterner is 4 m.

On the basis of preliminary experiments, with a view to the correct direction of the air-droplet flow to the treated object and capture of the working liquid, the fan-rotor spreading device is located at an angle of 22˚C. These parameters of the stand and the placement of the patterner were chosen in accordance with the parameters of the sprayed crops - orchards (fig. 2.6) and vineyards (fig. 2.7.)

The experiments were carried out at three different rotation frequencies of the fan-rotary spreading body -1400, 1800 and 2200 rpm and at 4 different flow rates 1.15; 2.3; 3.45 and 4.6 l/min.

The variation of the amount of liquid in the individual catch trays is determined by formula 2.1:

$$C = (\frac{x_i}{\bar{X}} - 1)100, \quad \% \quad (2.1)$$



Fig. 2.5 *The vertical patterner in action*

Where $\bar{X}$is the average amount of liquid in the collection tubes determined by expression:

$$\bar{X} = \frac{\sum \bar{x}_i}{n} \quad (2.2)$$

$\bar{x_i}$ – the amount of liquid in the $i^{\text{-тата}}$ test tube

n – number of tubes.

INVESTIGATION OF THE AIRFLOW PROFILE

The tests were carried out at 3 different distances of the patterner - 1, 2 and 3m from the fan-rotating spreader (fig. 2.6) in a windless room at 3 different rotation frequencies of the different fans - 1400 rpm, 1800 rpm, 2200 rpm. At these distances, a frame-net (fig. 2.7.) with dimensions 2x2.75m with shaped nodes located at a distance of 0.25 m from each other is placed. In these nodes, the speed of the air flow was measured using a point anemometer.

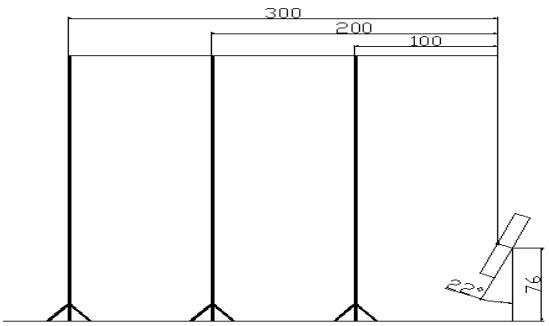


Fig. 2.6. Scheme of the air flow studies

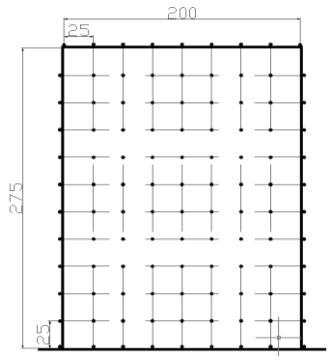


Fig. 2.7. An experimental network for the study of air flow velocity

Material provision for researching the quality of work of various spraying systems

The research was carried out at the "Nikola Pushkarov" ISSAPP - Sofia and covers the creation of the laboratory equipment, conducting the experiments, processing and analysis of the results.

The following instruments and devices were used in the experimental research: Measuring instrument for sensors “ALMEMO”; Air hygrometer; Tachometer (Sensor for measuring circular frequency); Anemometer (Sensor for measuring the speed of the air flow); Device for control and regulation of the vertical distribution of the working fluid (patternator); Water-sensitive paper.

Chapter 3. THEORETICAL STUDIES OF THE AIR DROP TORCH

3.1 Evaluation of the ecological-economic efficiency of pesticide use

At the moment, some of the least explored aspects in the research process are related to the systemic analysis and optimization of the technological and technical solutions used for plant protection. The degree of eco-economic efficiency of pesticide use can be assessed through the coefficient of useful utilization - ηp, which reflects the effective utilization of the quantity of pesticide formulations relative to the total amount of applied preparations, taking into account technological losses.

$$\eta_p = \frac{Q_{ta}}{Q_{to}}.100, \quad (3.1)$$

Where Q_{to} is the total amount of preparation per unit area.

$Q_{ta} = Q_{to} - \sum L_t/_H - \sum L_a/_H - \sum L_q/_H$ – Utilized purposefully on the treated area *H*.

The sum of losses $\sum L_t$, which depend on the technology of the operation, can be divided into:Losses related to the application of the working fluid and not hitting the target object (L_{tt}); Losses due to the evaporation of the working fluid (L_{tev}); Losses resulting from the working fluid landing on a non-target object (L_{te}); Losses caused by the acquisition of droplets from the treated object (L_{ti}); Losses due to an inadequate consumption rate relative to the degree of development of the treated object (L_{dd}); Losses resulting from changing meteorological conditions (rain, wind) (L_w).

$$\sum L_t = L_{tt} + L_{tev} + L_{te} + L_{tl} + L_{dd} + L_w. \quad (3.2)$$

The first component of these losses is related to drift and the transport of the working fluid outside the treated area. The amount of these losses primarily depends on the chosen method of droplet formation, the type of droplet spectrum, atmospheric conditions, and the treated object. Losses due to the carried-away spray from the treated area as an air-droplet mixture are caused by this mixture being deviated from the target under the influence of air currents. During its movement towards the treated object, some of the small droplets evaporate, while the larger droplets are prone to coalesce. Losses from droplets that do not hit the treated object are those that, when passing through the air-droplet plume through the vegetation, do not encounter leaf mass along their path and do not hit their intended target. These losses lead to the unintended deposition of the substances in other fields, water basins, and so on, resulting in additional losses.

The next three components reflect the excess contamination of the soil surface and the associated consequences. The final losses are related to the improper planning of a given operation or sudden changes in meteorological conditions. In the case of a sudden increase in wind or the onset of rain, there may be a forced suspension of the operation with no possibility of its recovery within acceptable timeframes.

The sum of losses $\sum L_a$ is related to auxiliary activities that are not directly connected to the treatment process. These losses are associated with the technology of pesticide storage (L_{as}), losses in the process of preparing the working fluid (L_{am}), losses in the process of transporting the working fluid (L_{at}), losses in the process of loading the sprayer with the working fluid (L_{ach}), and losses occurring in the process of cleaning transport vehicles, packaging, and sprayers (L_{ac}).

$$\sum L_a = L_{as} + L_{am} + L_{at} + L_{ach} + L_{ac}. \quad (3.3)$$

The sum of losses $\sum L_q$reflects the parameters of droplet coverage and the distribution of the working fluid when the applied working fluid on the treated object is not evenly distributed within the permissible deviation limits. Only the portion that falls within the requirements can be considered as purposefully utilized, while the remaining part is considered as loss. These losses

include those resulting from insufficient spraying (L_{qn}). This occurs when the spraying in terms of volume and quality is less than required to achieve a specific operation. In this case, the desired biological effect is not achieved. The other type of losses is from over-spraying (L_{qo}), meaning the amount of applied working fluid exceeds the normative allowable deviations. In this case, the desired effect is achieved, but at the cost of excessive consumption of the working fluid.

$$\sum L_q = L_{qn} + L_{qo}\,. \tag{3.4}$$

3.2. Movement of the droplet under the influence of the air flow

A droplet of the working fluid in the zone of action of the sprayer is subject to the forces generated by the air flow (Fw), the inertial forces (I) during its formation, and the force generated by the mass of the droplet (G).

$$F=G+F_w+I=m(g+a)+I, \tag{3.5}$$

Where m is the mass of the droplet in kilograms (kg),

g is the gravitational acceleration in meters per second squared (m/s²),

and a is the acceleration imparted to the droplet by the air flow in meters per second squared (m/s²).

From the literature, it is known that the acceleration imparted to a droplet by an air stream is determined as follows [3]:

$$a = \frac{c \cdot \rho_в \cdot S_к \cdot V_в^2}{m}, \tag{3.6}$$

Where c is the coefficient of air resistance,

$\rho_в$- is the air density in kilograms per cubic meter (kg/m³),

$S_к$ is the cross-sectional area of the droplet in square meters (m²),

$V_в$ is the velocity of the air flow in meters per second (m/s),

m is the mass of the droplet in kilograms (kg).

The coefficient of air resistance depends on the Reynolds number and is determined by the formula [4]:

$$c = \frac{24}{Re} + \frac{2.5}{\sqrt[4]{Re}}, \tag{3.7}$$

Where $Re = \frac{V_в \cdot d_к}{v}$ is the Reynolds number,

$d_к$ is the diameter of the droplet in meters (m),

v is the kinematic viscosity of the air (ν =1,45 × 10^{-5} m^2/s at 20°C).

We consider the droplet in the stationary coordinate system XY connected to the sprayer (Fig. 3.1). It is positioned perpendicular to the ground. We examine the forces acting on a given droplet in two opposite positions in the plume. We idealize the direction of the air flow, assuming the center of the fan as its source. Under these assumptions, the general form of the differential equation for the motion of the droplet can be written as:

$$m \cdot \frac{V'}{dt} = (mg + ma) + I \tag{3.8}$$

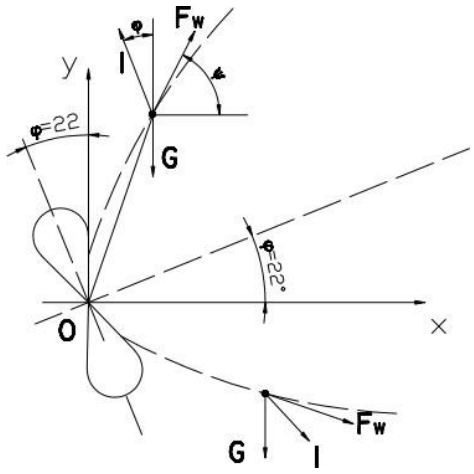


Fig. 3.1. Diagram of the forces acting on the droplet in the idealized view of the process of its movement.

$$m_i \frac{d^2 X_i}{dt^2} = \sum_{i=1}^{n} \overrightarrow{F_w} + \vec{I} + \vec{G} \tag{3.9}$$

$$\begin{cases} m\ddot{x} = \sum_{i=1}^{n} \pm G_x \pm F_{w_x} \\ m\ddot{y} = \sum_{i=1}^{n} \pm G_y \pm F_{w_y} \end{cases} \tag{3.10}$$

$$\begin{cases} m\ddot{x} = \sum_{i=1}^{n} m\left(\pm \frac{c \cdot \rho_в \cdot S_к \cdot V_в^2}{m} sin\varphi\right) + \frac{L}{\omega} \\ m\ddot{y} = \sum_{i=1}^{n} m\left(\pm g sin\theta \pm \frac{c \cdot \ddot{\rho}_в \cdot S_к \cdot V_в^2}{m} cos\varphi\right) + \frac{L}{\omega} \end{cases} \tag{3.11}$$

Where L is the angular momentum and ω is the angular velocity of the sprayer.

3.3. Movement of the droplets after leaving the sprayer

The general form of the differential equation for the motion of the i[тата] droplet can be written as:

$$m_i \frac{dV_i}{dt} = \vec{G}_{ki} + \vec{F}_{ki} \tag{3.12}$$

Where m_i is the mass of the i[тата] droplet in kilograms (kg),

V_i is the velocity of motion of the i-th droplet in meters per second (m/s).

The weight of the droplets is calculated using the formula:

$$G_{ki} = \frac{4}{3}\pi r_i^3 \gamma_w \, , \tag{3.13}$$

Where $r_i$is the radius of the i[тата] droplet in meters (m),

γ_w is the volumetric weight of water in newtons per cubic meter (N/m³).

The force generated by the air flow created by the fan acting on the i[тата] droplet can be calculated using the expression:

$$F_{ki} = \frac{1}{2} C_x \rho_a V_{ki}^2 S_{ki} \tag{3.14}$$

$C_x$is the coefficient of resistance of the moving droplets,

ρ_a is the air density in kilograms per cubic meter (kg/m³),

S_{ki} is the frontal surface area of the i-th droplet in square meters (m²).

After several transformations and integration for the motion of the i-th droplet, the expression is obtained as follows:

$$\begin{cases} X_{ki} = \frac{V_{koi} cos\alpha_i}{k_1}(1 - e^{-k_i t}) \\ Y_{ki} = h_Д - R_Д cos\alpha_i + \left(\frac{V_{koi} sin\alpha_i}{k_1} - \frac{k_2}{k_1^2}\right)(1 - e^{-k_i t}) + \frac{k_2 t}{k_1} \end{cases} \tag{3.15}$$

3.4. Determination of the theoretically required consumption of the working fluid.

The theoretically required consumption of the working fluid for conducting a specific operation can be determined by taking into account the area of the treated object, the average volumetric diameter of the droplet spectrum, the leaf area index, agrotechnical requirements for droplet coverage density, and the losses of the working fluid.

$$Q = \frac{SL_i n(1-k)D_v^3}{\eta} \quad (3.16)$$

Where:

S is the treated object's surface area per hectare in square meters per hectare (m^2/ha).

L_i is the leaf area index.

n is the density of droplet coverage according to agrotechnical requirements, drops per square centimeter (drops/cm^2).

k is the ratio of the density of droplet coverage on the back to the front side.

D_v is the average volumetric diameter of the droplets in millimeters (mm).

η is the percentage of working fluid effectively utilized for its intended purpose, %.

η is calculated as follows:

$\eta = 100 - \eta_d - \eta_e - \eta_{nt} - \eta_{fd}$,

Where:

η_d is the percentage of the working fluid carried away as an air-droplet mixture.

η_e is the percentage of losses due to evaporated droplets of the working fluid.

η_{nt} is the percentage of losses from droplets that do not hit the treated object.

η_{fd}, is the percentage of losses due to droplet coalescence.

Pesticide application rates are typically given per unit area. The actual treated area can vary with the development of the treated object, the crop variety, and the cultivation technology.

The actual application rate of the pesticide (R) can be determined based on the formula:

$$R = R_{et}. k_r, \quad (3.17)$$

Where R_{et} is the label dose of the product, and k_r is the reduction coefficient.

The reduction coefficient will depend on specific conditions, the treated object, the requirements of the pest control being carried out, and the conditions under which the application rate was determined.

The optimization task consists of justifying an application rate that achieves effective plant protection with minimal ecological consequences and financial expenses. Figure 3.2 shows the strong influence on the application rate of the degree of development of perennial plantations and the diameter of the droplets used. The latter parameter depends on the capabilities of the equipment used. On the other hand, the technological requirement for droplet coverage density, as shown in Figure 3.3, must also be met. Based on the graphical interpretation of the dependencies, the application rate can be planned depending on the recommended density, droplet diameter, and plant development specific to the given operation.

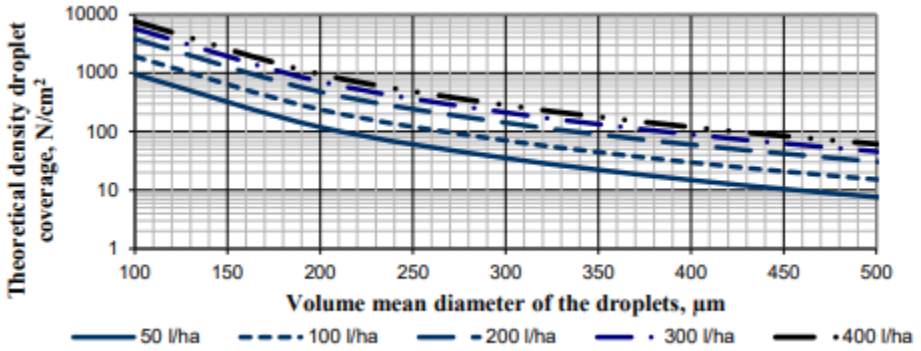


Fig. 3.2. The theoretically achieved droplet coverage density as a function of droplet diameter at different application rates of the working fluid.

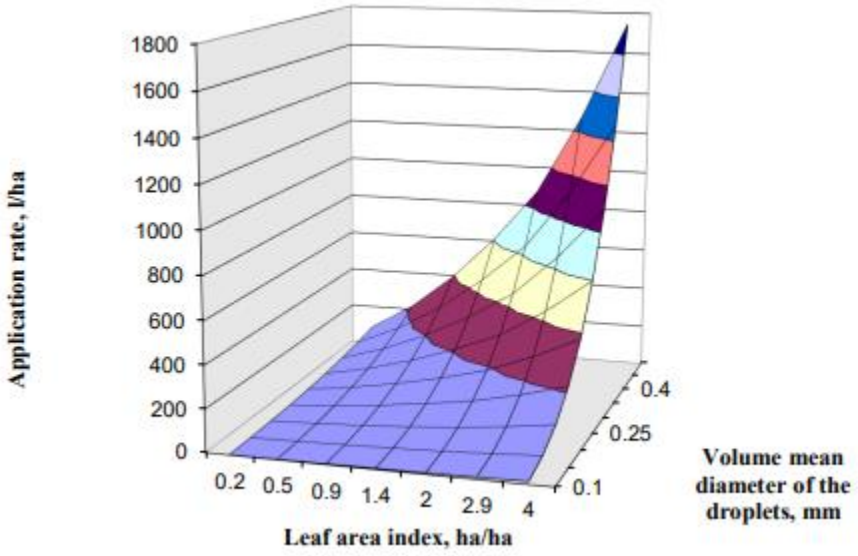


Fig. 3.3. Dependency of the application rate of the working fluid on the leaf area index and droplet diameter.

3.5. Analysis of Droplet Prints

The analysis of droplet prints, used to assess the parameters of the droplet spectrum, is carried out with a program developed by us in C++.

Procedure

The droplet prints are obtained on a medium, which can be various types of paper - white or water-sensitive, with a known or determined spreading coefficient. The paper sheets are scanned on a scanner with a specified sensitivity, which is set in the program for the correct calculations.

Algorithm

The scanned image is saved as a grayscale image in Bitmap Image format (.bmp). The program reads the image and creates a two-dimensional array with information for each pixel of the image. The main information for each pixel is its position in the array (coordinates) and the grayscale depth. The grayscale depth varies from 0 - pure black to 255 - pure white. Depending on the sensitivity, which can be set in the program, the output results change - the size and number of images (droplets). Fig. 3.4 shows a general view of an image of droplet prints and a window where settings related to the image analysis can be made. Essentially, these are filters that can be used to determine optimal values for each image to determine the parameters of the droplet coverage. These are grayscale depth, which is done with the upper slider, and below it is the setting that determines the ellipticity of a given print. The largest and smallest diameter of a given print is determined, and based on this, the ratio between them is calculated. It is usually assumed that a given print is the work of only one droplet if the ratio between the large and small diameter is maximally ½. The operator can also select a smaller ellipticity. Another input parameter is the resolution of the image - Dpi. Depending on the surface on which the droplet prints are collected, the spreading coefficient is selected. When using water-sensitive paper, the coefficient is calculated using the formula shown in the window.

Once the image is loaded and the necessary settings are made, the analysis process begins. The image is examined as an array.

i - coordinate on the abscissa

j - coordinate on the ordinate

The analysis starts from the upper left corner with coordinates A(i, j). The array is traversed until an element with grayscale depth greater than that set by the operator Aij <h is found, which means an element that stands out from the background. When such an element is found, the traversal of its adjacent elements begins in order to localize and record the elements that make up the entire spot. Fig. 3.5 shows the general view of two droplets of different sizes and the structural view of the elements that make up the droplet print.

Traversing the print is done recursively by checking all elements up to the current one. Each traversed element is marked so that it is not processed again. When the program recursively traverses all adjacent elements with grayscale depth greater than the set one, the obtained information for the given droplet is recorded. The analysis continues as all the other elements of

the array are traversed. When a new element with grayscale depth greater than the set one is found, the algorithm repeats.

The analysis ends when all elements of the array are traversed. The program allows for visualization of the droplet prints reported at a given grayscale level. This allows you to search for the most suitable level according to the background.

Based on this information, the area of each print is calculated.

$$S=n.Sn, \quad mm \tag{3.19}$$

where n is the number of elements within a given spot;

Sn – the area of one element.

$$Sn=(25.4/Dpi)2, mm2 \tag{3.20}$$

From which, for the diameter of the i-rata droplet, we obtain:

$$D_i=\sqrt{(4S/\pi)}, \quad mm. \tag{3.21}$$

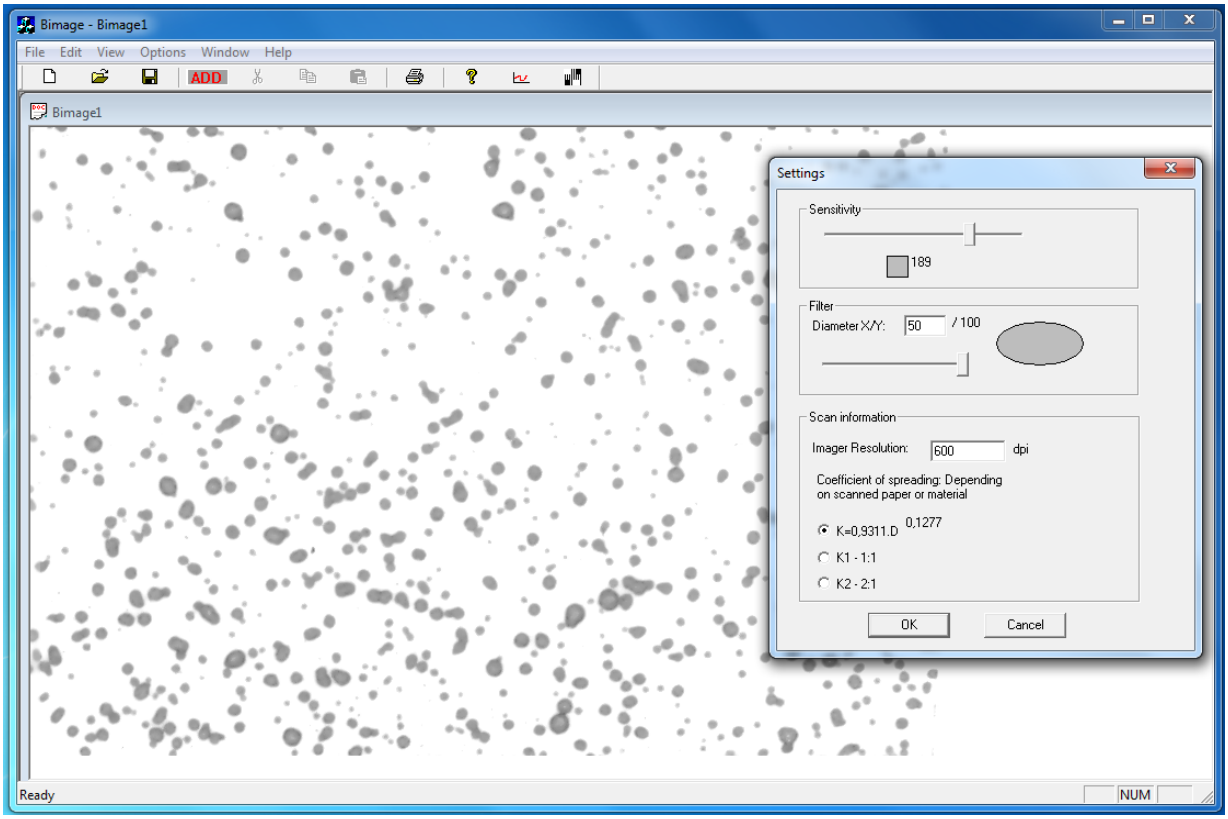


Figure 3.4. General view of the image of droplet imprints with the adjustment window

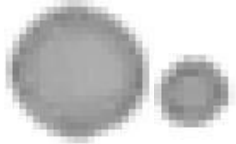


Figure 3.5. General view of droplet imprints

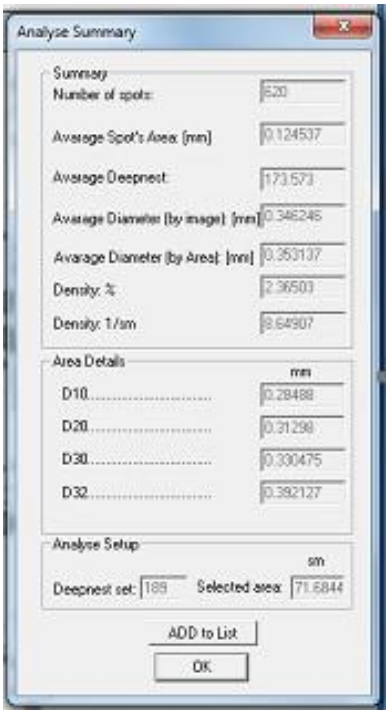


Figure 3.6. Results of the analysis of a given test sheet.

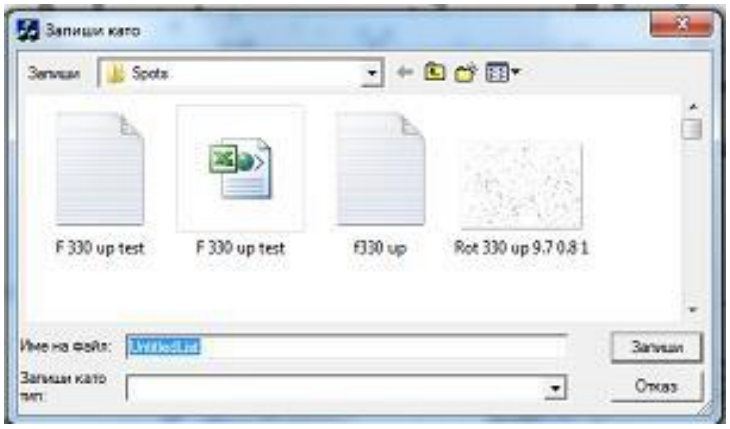


Figure 3.7. Saving the results obtained for a specific test sheet in an Excel file.

When the option to display the obtained results is activated, the window shown in Figure 3.6 opens. There is also the possibility to import these results into an Excel file for further processing and analysis, as shown in Figure 3.7. This way, the results obtained from different test sheets can be combined and processed together.

Chapter 4. RESULTS AND ANALYSIS OF EXPERIMENTAL STUDIES

4.1. Results of the Airflow Profile Investigations

Airflow Profile of a 500 mm Diameter Fan

Figure 4.1 presents a 3D profile of the airflow obtained from a 500 mm diameter fan operating at 1400 rpm, measured at a distance of 1 meter. The profile exhibits a bimodal shape in the vertical direction and a unimodal shape in the horizontal direction (Figure 4.2).

It can be observed that at a height of 1.25 meters, the air velocity reaches 8 m/s. In the horizontal direction, the profile illustrates the possibility of gradually increasing the airflow velocity, in this

case, up to 5.5 m/s, during the linear movement of the machine. This allows for a smooth rotation of the leaf canopy of the treated object. The cross-sections were made in two mutually perpendicular planes centered on the measurement grid.

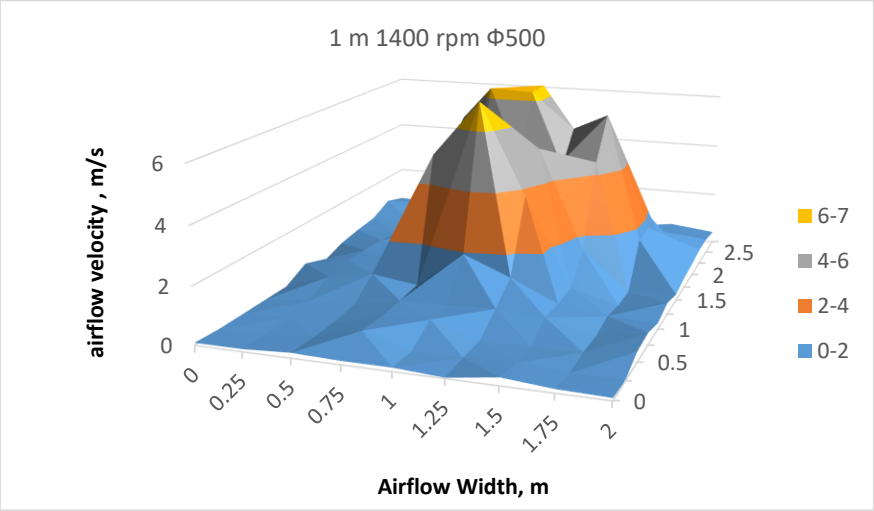


Figure 4.1. Airflow profile at a distance of 1 meter from the fan at a rotation speed of 1400 rpm.

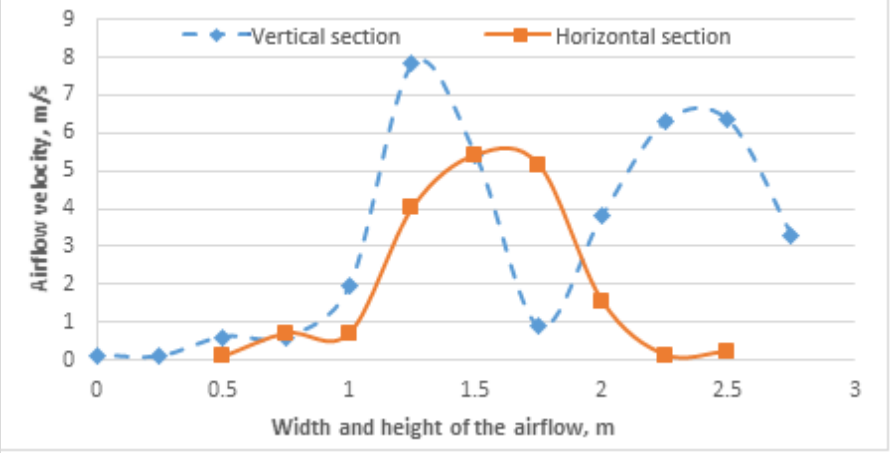


Figure 4.2. Cross-section of the airflow at a distance of 1 meter from the fan at a rotation speed of 1400 rpm. As the distance from the fan increases (Figure 4.3), the bimodality of the profile in the vertical section is maintained, but the maximum values decrease and have equal values in both sections (Figure 4.4). The airspeed in this section does not exceed 6 m/s. There is a larger decrease in the size of the second peak compared to the first one.

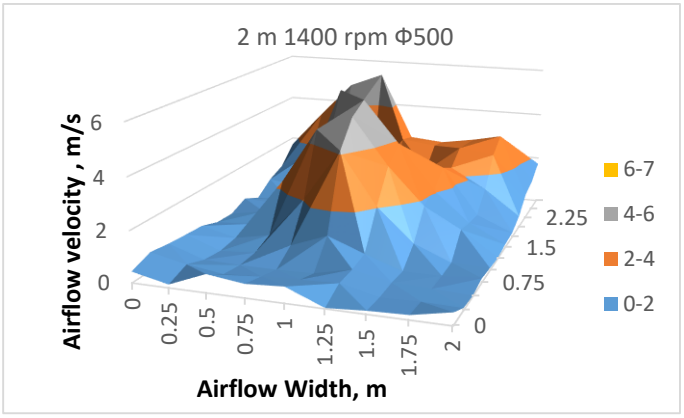


Fig. 4.3. Airflow profile at a distance of 2 m and a rotation speed of 1400 rpm.

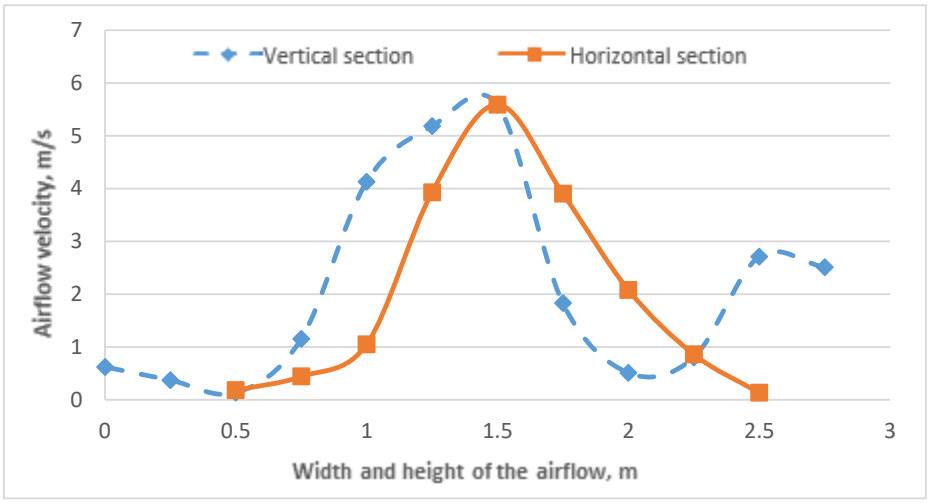


Fig. 4.4. Cross-section of the airflow at a distance of 2 m and a rotation speed of 1400 rpm

At the same fan with a 500 mm diameter and a rotation speed of 1800 rpm, at a distance of 1 m from the fan, the airflow profile has the same shape as at 1400 rpm - bimodal in the vertical section and unimodal in the horizontal section (Fig. 4.5 and 4.6). The airflow velocity reaches 9 m/s at heights of 1.5 m and 2.25 m.

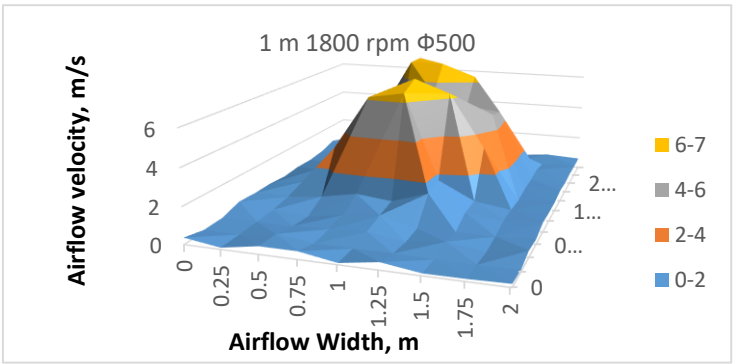


Fig. 4.5 Airflow profile at a distance of 1 m and a rotation speed of 1800 rpm

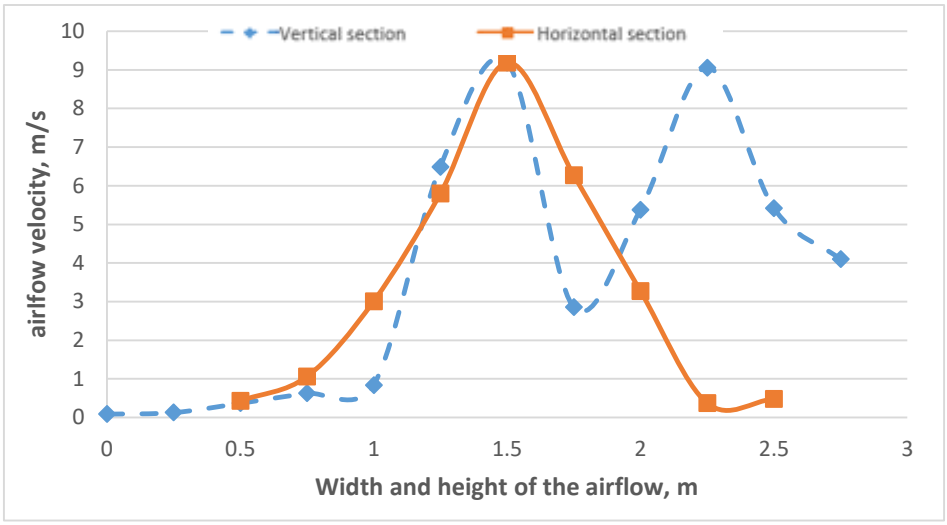


Fig. 4.6. Cross-section of the airflow at a distance of 1 m and a rotation speed of 1800 rpm

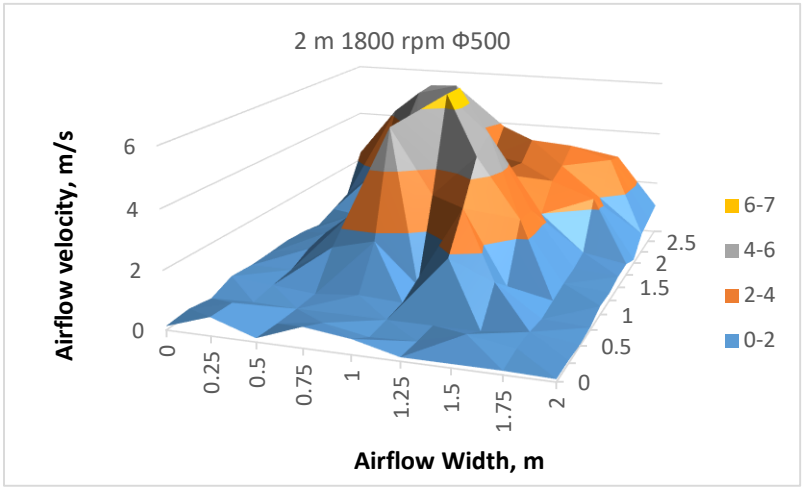


Fig. 4.7. Airflow profile at a distance of 2 m and a rotation speed of 1800 rpm

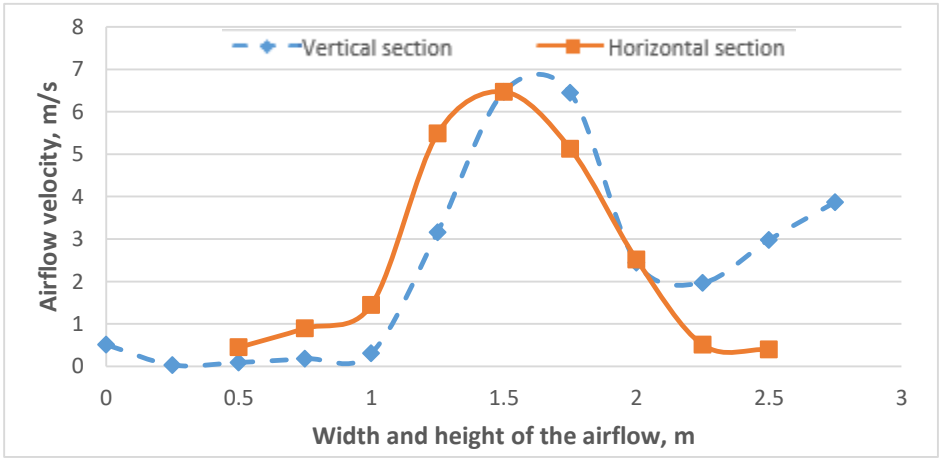


Fig. 4.8. Cross-section of the airflow at a distance of 2 m and a rotation speed of 1800 rpm

And at this rotation speed, with an increase in the distance from the fan, the bimodality of the vertical distribution transitions even faster into unimodality (Fig. 4.7 and 4.8). However, the decrease in the peak velocity at a height of 1.4 m occurs at the same rate.

The airflow velocity exhibits the same characteristics at a fan speed of 2200 rpm, as it does at the previous two fan speeds. At a distance of 1 m, the peak airflow velocity reaches 12 m/s, at 2 m – 9 m/s, and at 3 m – 5.5 m/s. From the obtained results, it can be observed that at all three fan speeds for a 500 mm diameter fan, the shape of the airflow profile is similar at all three distances from the fan. In the horizontal cross-section through the center of the plume, the velocity graph retains its unimodal shape, while in the vertical cross-section, it changes from bimodal at 1 m from the fan to unimodal at 3 meters. The maximum velocity is achieved at heights of 1.25-1.5 m in all three modes and distances. It can be seen (Fig. 4.9) that the dependence of the maximum airflow velocity on the change in fan speed has a similar character at all distances from the fan.

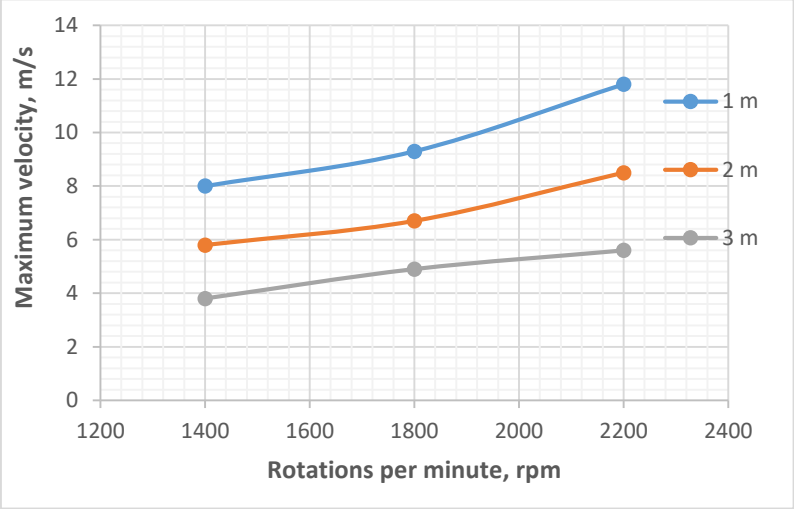


Fig. 4.9. Variation in the maximum airflow velocity at different distances from the 500 mm diameter fan at different fan speeds

Profile of the airflow from a 600 mm diameter fan, modification M1

Figure 4.10 shows the profile of the airflow at a distance of 1 m and a fan speed of 1400 rpm. In this fan model, which is rotationally modified, the airflow velocity profile does not exhibit a clear modal form as seen in the 500 mm diameter fan. In the vertical cross-section at this operating mode, the airflow velocity starts to increase above a height of 1 m, with nearly uniform velocity around 5 m/s from a height of 1.5 m to 2.75 m, as shown in Figure 4.11.

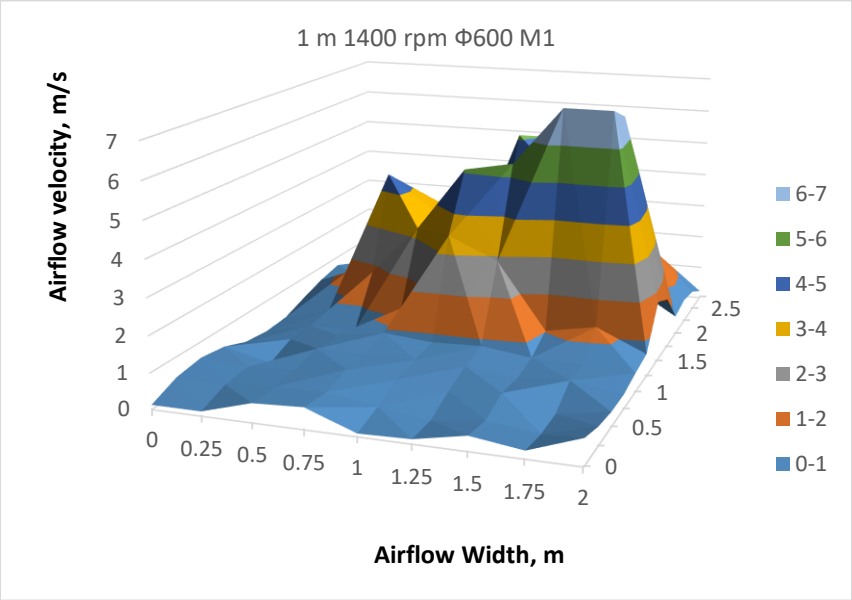


Figure 4.10. Airflow profile at a distance of 1 m and a fan speed of 1400 rpm

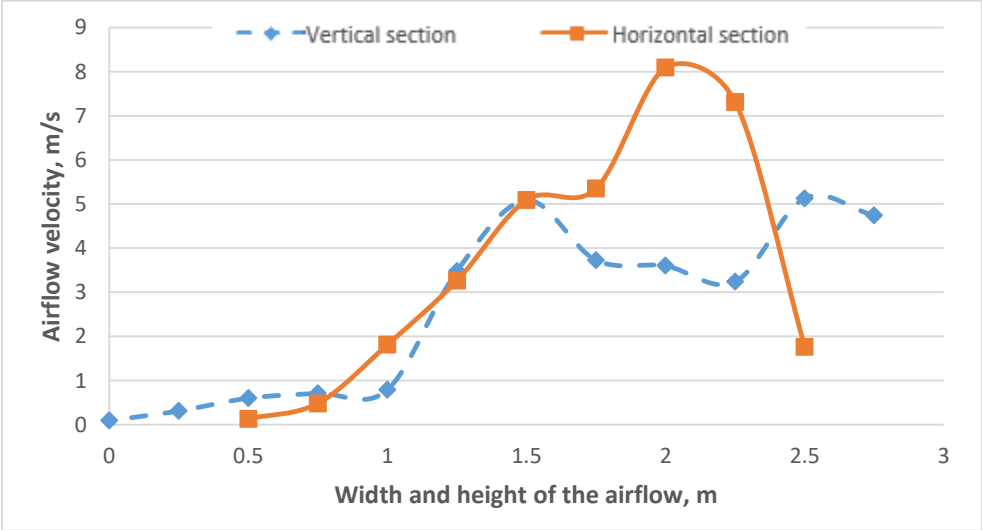


Figure 4.11. Cross-section of the airflow at a distance of 1 m and a fan speed of 1400 rpm

With an increase in distance from the fan to 2 m, the character of the airflow profile remains the same (Figures 4.12 and 4.13). The same applies to its horizontal section, with its maximum value reaching 4.5 m/s. In the vertical section, the speed reaches 3.5 m/s, with the increase starting at a height of 1 m, and after 1.5 m, it remains in the range of 3 to 3.5 m/s.

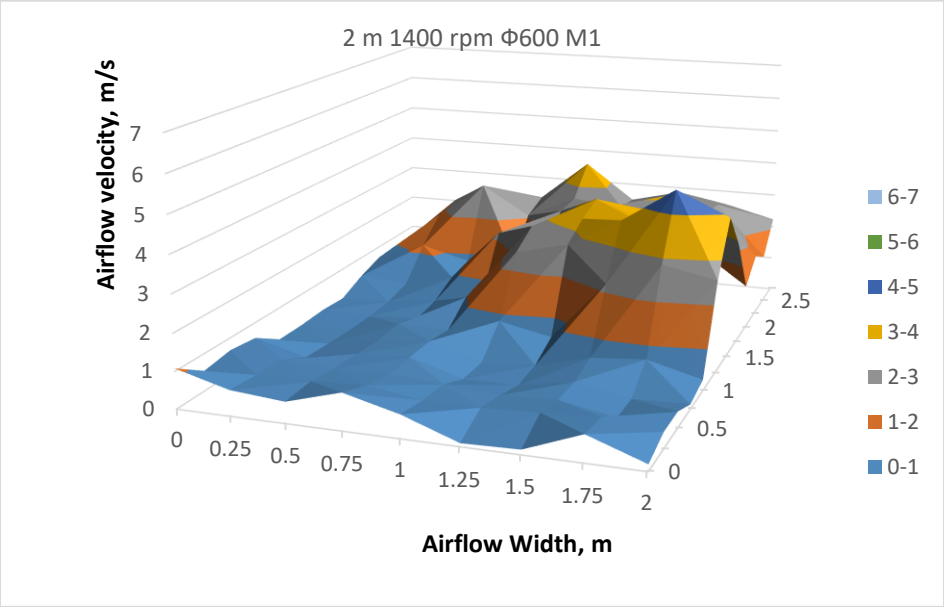


Figure 4.12. Airflow profile at a distance of 2 m and a rotational speed of 1400 rpm

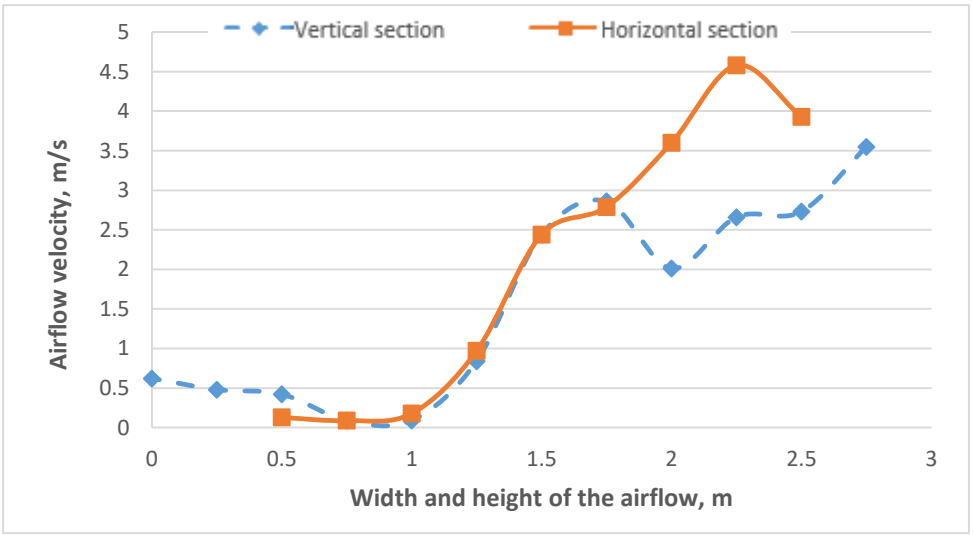


Figure 4.13. Cross-section of the airflow at a distance of 2 m and a rotational speed of 1400 rpm.

The logical trend continues as the distance increases to 3 m. The maximum airflow velocity at the vertical section reaches 2.8 m/s at a height of 2.5 m. Then, it starts to decrease to 1.5 m/s at a height of 2.72 m. In the horizontal direction, the maximum airflow velocity reaches 3.2 m/s.

With an increase in the rotational speed of this fan model, the airflow profile at a distance of 1 m from the fan becomes more diverse, as shown in Figure 4.14. The maximum velocity (7.2 m/s) at the central vertical section is achieved at a height of 1.25 m. In the horizontal section, the maximum velocity reaches 10 m/s.

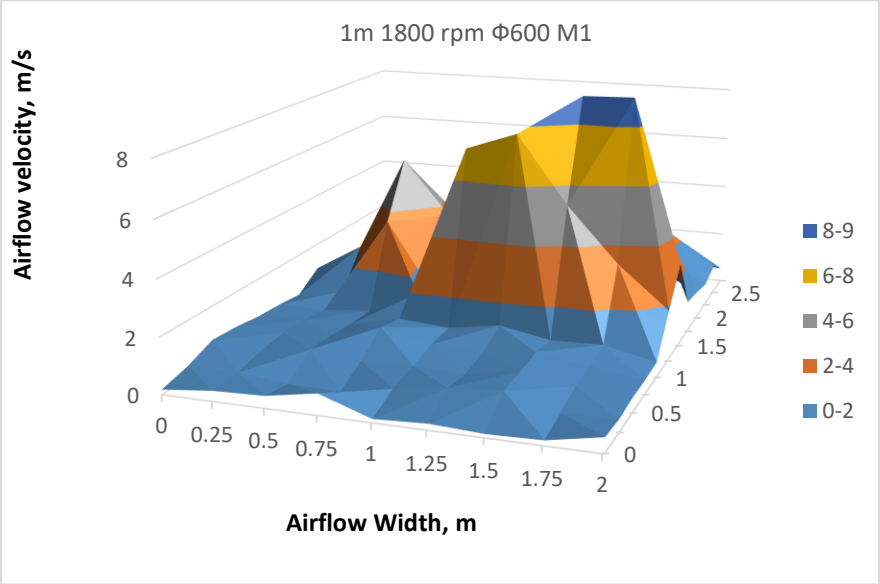


Figure 4.14. Airflow profile at a distance of 1 m and a rotational speed of 1800 rpm

With an increase in the distance from the fan to 2 m, the general characteristics of the airflow profile are maintained (Figure 4.15), with speeds reaching around 3 m/s from 1.5 m to 2.75 m in height. In the horizontal section, the speed is above 6 m/s. At the central point of the profile, the airflow speed is 3.25 m/s.

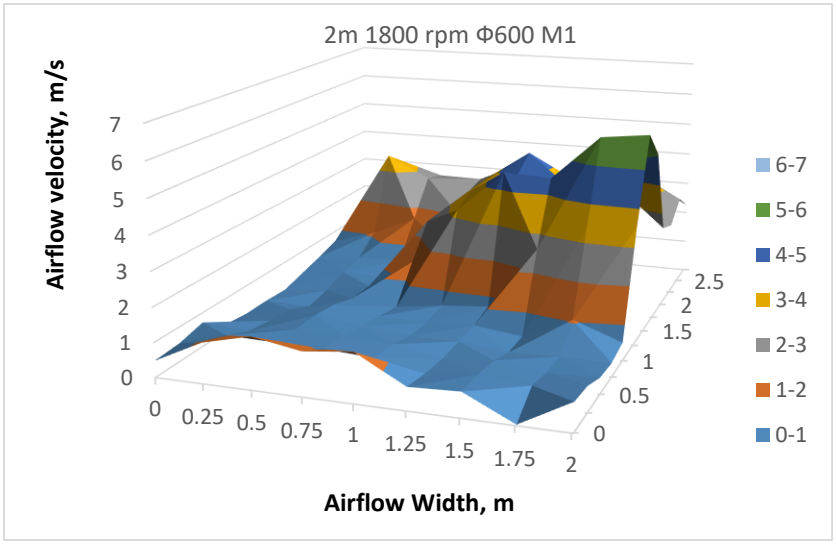


Figure 4.15. Airflow profile at a distance of 2 m and a rotational speed of 1800 rpm

The character of the change in the maximum airflow velocity with an increase in the rotational speed when using a 600 mm diameter fan, modification M1 (Figure 4.16), is similar to that of a 500 mm diameter fan. The difference lies in the faster decrease in the maximum velocity with an increase in distance from the fan. Here, too, the increase in airflow velocity in the horizontal section is relatively smooth. This creates conditions for the smooth swirling of the leaf and fruit mass and their uniform spraying.

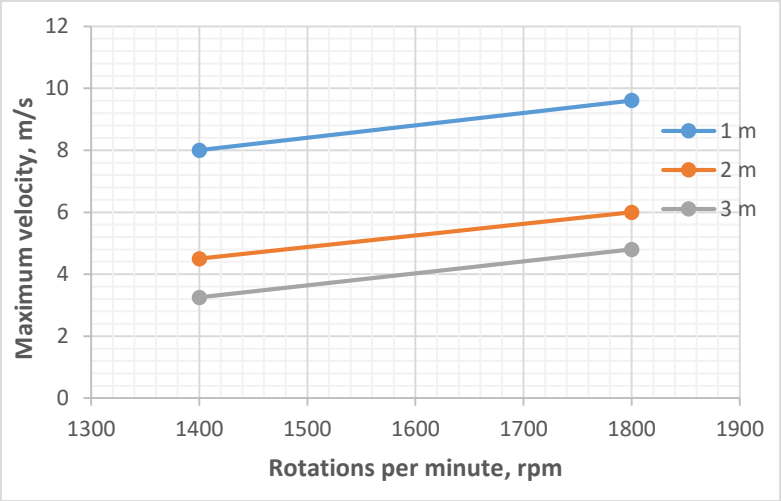
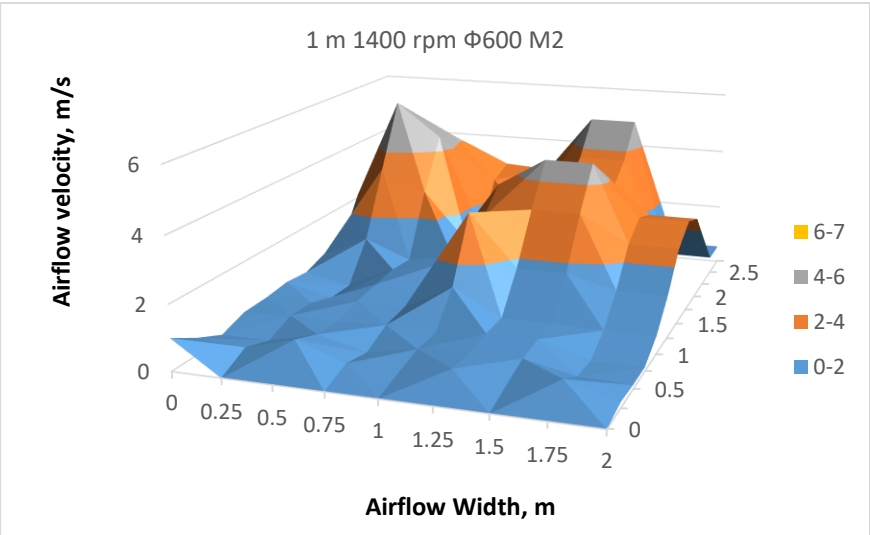


Figure 4.32. Change in the maximum airflow velocity at different distances from the 600 mm diameter fan, modification M1, at various rotational speeds

Figure 4.17 shows the airflow profile at a distance of 1 meter from the 600 mm diameter fan with modification M2. The profile is similar to that of modification M1. However, unlike M1, this modification exhibits two peaks in airflow velocity. Above 1 meter in height, the airflow velocity increases from 1 m/s to 6 m/s at a height of 1.75 m, and it does not drop below 3 m/s in the range up to 2.75 m.

As the distance from the fan increases to 2 meters, the shape of the airflow profile (Figure 4.18) becomes unimodal, and the velocity reaches 4.8 m/s. The maximum velocity (4.8 m/s) is at the



center of the profile, at the intersection of the vertical and horizontal cross-sections of the profile, as shown in Figure 4.35. Starting from a height of 0.8 meters, the airflow velocity increases from 1 m/s to 4.7 m/s at a height of 1.5 meters and then decreases to 1.3 m/s at a height of 2.5 meters.

Figure 4.17. Airflow profile at a distance of 1 meter and a rotational speed of 1400 rpm

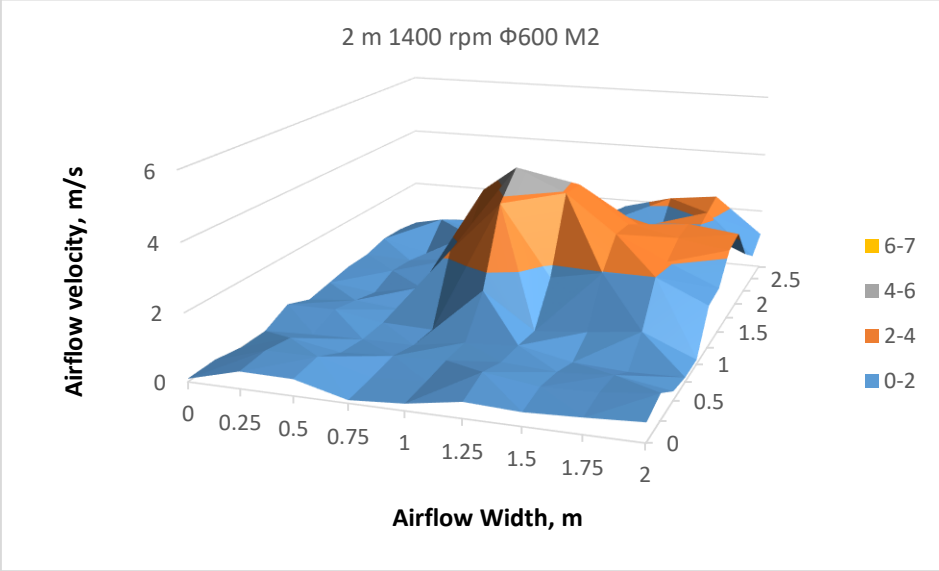


Figure 4.18. Airflow profile at a distance of 2 meters and a rotational speed of 1400 rpm

The single-modal character of the airflow profile is maintained up to a distance of 3 meters from the fan, with the maximum speed reaching up to 3.8 m/s. The maximum speed value in the vertical section through the center of the plume is 3.5 m/s. Starting from a height of 1 meter and an airflow speed of 1 m/s, the speed increases to 3.5 m/s at a height of 1.75 meters, after which it decreases relatively slowly to 1.75 m/s at a height of 2.75 meters.

Figure 4.19 shows the airflow profile at a distance of 1 meter and a fan rotational speed of 1800 rpm. For this fan model with rotational dispersion, the profile of airspeed does not have a clearly defined modal shape, as seen with the 500 mm diameter fan, modification M1. In the vertical section at this mode, the airspeed starts to increase above a height of 1 meter. It increases to 5.8 m/s up to a height of 1.75 meters and decreases to 2.5 m/s at 2.75 meters.

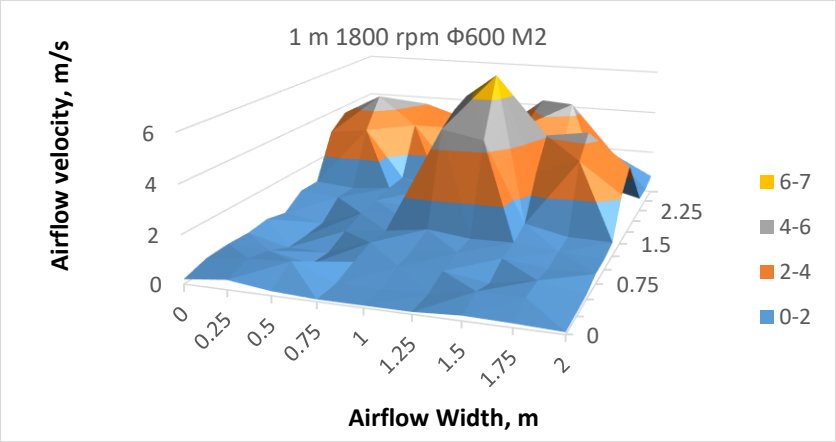


Figure 4.19. Airflow profile at a distance of 1 meter and a rotational speed of 1800 rpm

As the distance from the fan increases to 2 meters, the shape of the profile remains the same while the airflow velocity decreases (Figure 4.20), with the maximum velocity being 4.6 m/s. In the vertical section of the airflow profile, velocities are below 1 m/s up to a height of 1 meter, then they increase to 3.3 m/s at a height of 1.5 to 2.25 meters, and subsequently decrease to 1 m/s at a height of 2.75 meters.

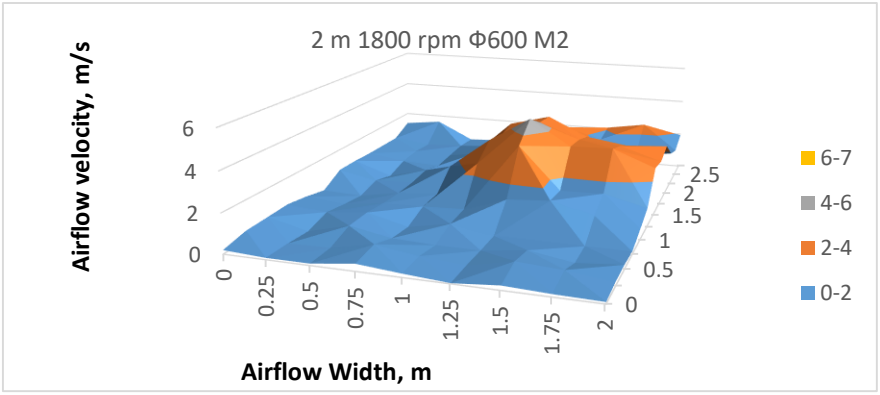


Figure 4.20. Airflow profile at 2 meters distance and 1800 rpm rotation speed

The airflow profile, upon reaching a distance of 3 meters from the fan, takes on a more clearly defined centrally located unimodal shape. The maximum speed is at the intersection point of the vertical and horizontal cross-sections (1.5 meters) and is 3.9 m/s. It can be seen that it exceeds 1 m/s for all heights above 1 meter, which is a prerequisite for spraying the plant material above this height.

The nature of the change in maximum airflow speed with increasing rotation speed when using a 600 mm diameter fan, modification M2 (Figure 4.21), is similar to that of the M1 modification. Here as well, the increase in airflow speed in the horizontal cross-section is relatively smooth. This creates conditions for the gentle swirling of leaf and fruit material and avoids the creation of a "wall," ensuring uniform spraying.

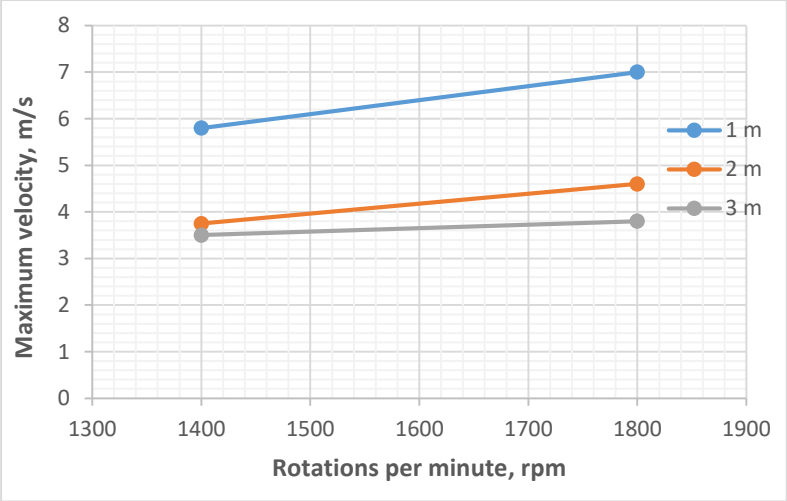


Figure 4.21. Variation of the maximum airflow speed at different distances from the 600 mm diameter fan, modification M2, at various rotation speeds

Figure 4.22 shows the change in the average velocity of the airflow profile of the 500 mm diameter fan. Different gradients of the average velocity can be observed with increasing distance from the fan. The smallest decrease in velocity with increasing distance from the fan occurs at a rotation speed of 1800 rpm. This makes this mode recommended for operation with this fan.

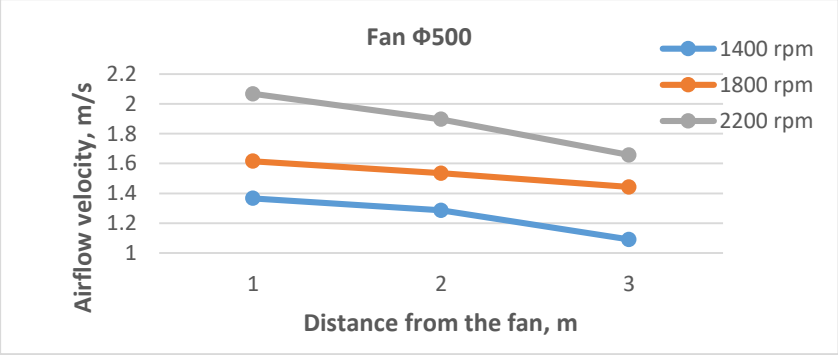


Figure 4.22. Change in average airflow velocities for a 500 mm diameter fan at various distances.

On Figure 4.23, the change in average airspeeds using the 600 mm diameter fan model M1 is shown. It is clearly noticeable that the average speeds decrease more rapidly at both rotation speeds as the distance from the fan increases for this fan compared to the 500 mm diameter fan.

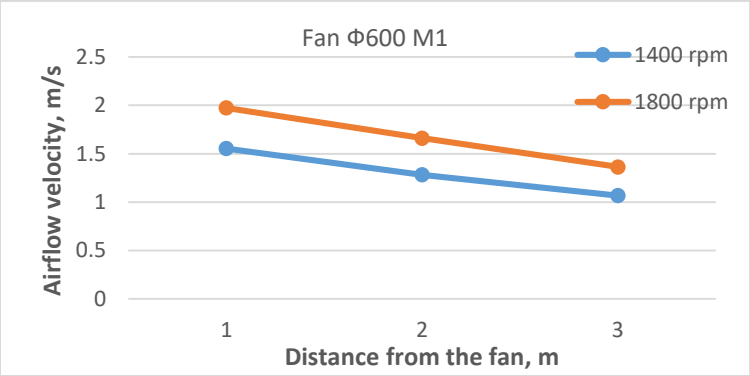


Figure 4.23. Change in average airspeeds with a 600 mm diameter fan model M1 at various distances

Figure 4.24. Change in average airspeeds with a 600 mm diameter fan model M2. It can be seen that with this fan modification, the average speed is practically independent of the rotation frequency and is less affected by the distance. This highlights the importance of the blade shape on the airflow parameters.

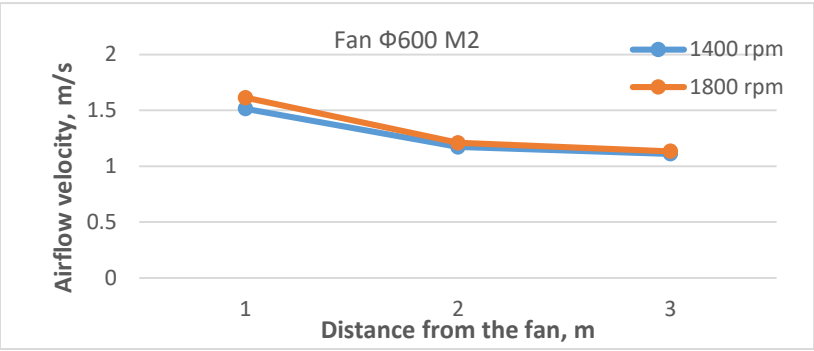


Figure 4.24. Change in average airspeeds with a 600 mm diameter fan model M2 at different distances.

4.2. Results of Investigations on the Distribution of the Working Fluid

Results of the investigations on the distribution of the working fluid with a 500 mm diameter fan-rotational nozzle

Figure 4.25 shows the relative distribution of the working fluid at a distance of 1 m from the fan at different rotation speeds.

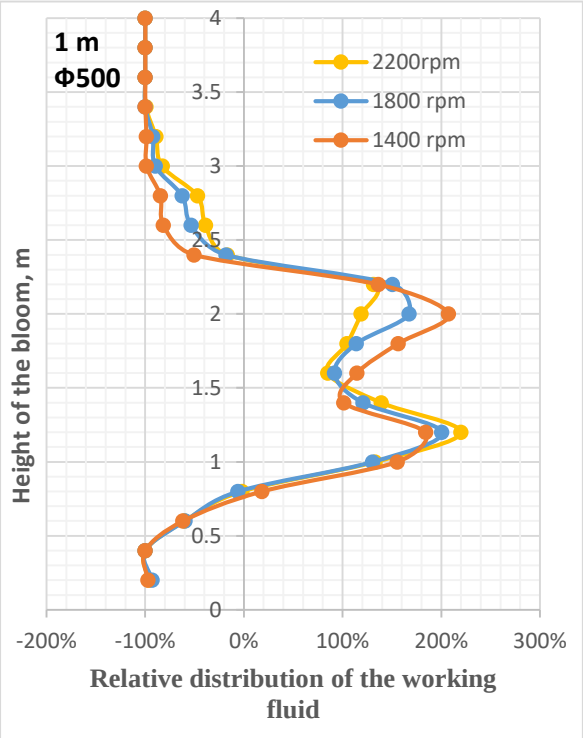


Figure 4.25. Relative distribution of working fluid at a distance of 1 meter from the 500 mm diameter fan

It can be seen that the working fluid is mainly concentrated in the zone from 0.8 to 2.4 meters. In this zone, the distribution has two peaks. To a very small extent, this distribution is influenced by changes in the rotational speed. To some extent, at the peak height of 2 meters, a decrease in rotational speed increases the amount of working fluid. This is likely due to larger droplets concentrating in this zone at low rotational speeds.

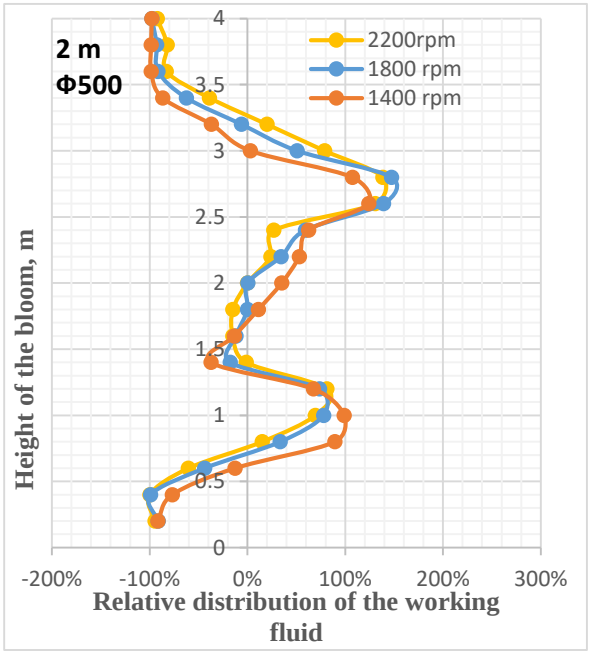


Figure 4.26. Relative distribution of the working fluid at a distance of 2 meters from the 500 mm diameter fan

At a distance of 2 meters from the sprayer, the shape of the working fluid distribution is also bimodal, weakly influenced by the fan's rotation speed (Figure 4.26). In this case, the two peaks decrease in size and become more separated in height.

The lower peak decreases slightly in height, while the upper peak shifts upward to around 2.7 meters. At a distance of 3 meters from the working device, the scattering of the distribution in height decreases. It continues to maintain its bimodal shape but with less difference. The decrease in peak heights progressively with increasing distance from the sprayer, from 210% at 1 meter to 150% at 2 meters and 110% at 3 meters, is likely due to the influence of turbulence in the carrying airflow. For this fan diameter, the average value of the root mean square deviation of the relative distribution of the working fluid increases from 7% to 14% when the distance from the fan increases from 1 to 3 meters.

Results of the study on the distribution of the working fluid for the fan with a 600 mm diameter and fan modification M1:

Figure 4.27 shows the curves of the relative distribution of the working fluid at a distance of 1 meter from the fan with a 600 mm diameter and fan modification M1. In this fan model, the curves are also bimodal, but the upper peak is much smaller in size and at a greater height compared to the fan with a 500 mm diameter. The lower peak is at the same height for both fans and is larger for the lower rotation speed, being 100% larger than the same mode for the 500 mm diameter fan.

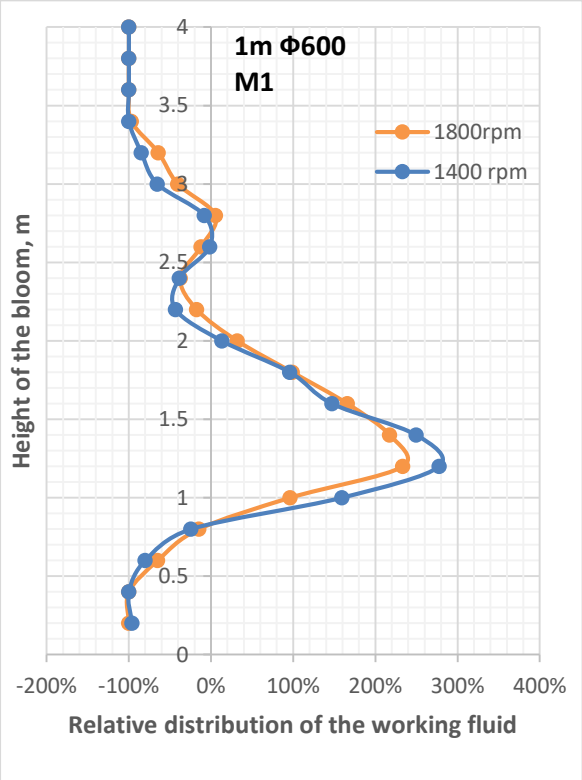


Figure 4.27. Relative distribution of the working fluid at a distance of 1 meter from the fan with a 600 mm diameter, model M1

A similar pattern is also observed in the distribution curves for this fan at a distance of 2 meters (Figure 4.28). However, at 3 meters, the lower peak decreases to 200%, and the distribution itself is highly variable but gradually decreases overall from a height of 1.25 meters.

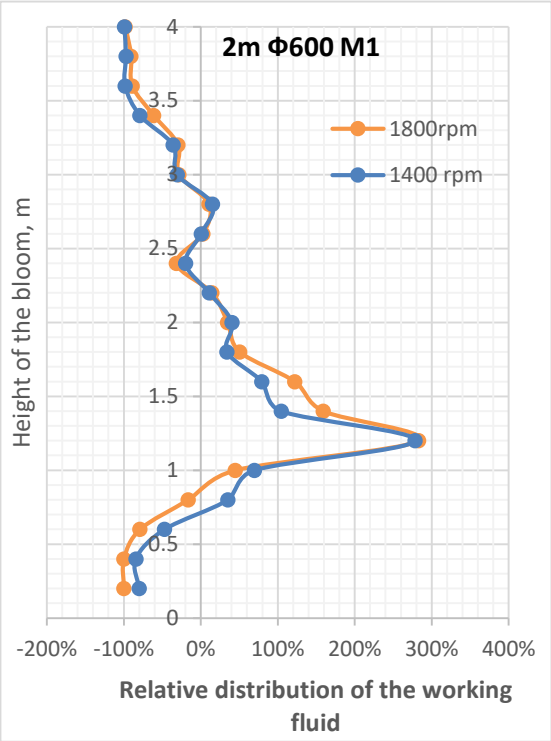


Figure 4.28. Relative distribution of the working fluid at a distance of 2 meters from the 600 mm diameter fan, model M1.

Results from the investigation of the distribution of the working fluid in the fan rotation spray nozzle with a 600mm diameter and the M2 fan modification

For the 600mm diameter Model M2 fan (Figure 4.29), at a distance of 1 meter, the relative distribution of the working fluid is similar in character to that of the 600mm diameter Model M1 fan at 3 meters from the fan. However, the peak is 100% larger, and in this fan model with seven blades, the distribution is unimodal, unlike the 500mm diameter fan, where it is bimodal. This suggests that the shape of the air plume formed by the three different spray devices, with varying diameters and numbers of blades, has a different impact on the distribution of the working fluid by height. As the distance from the fan increases (Figure 4.29 and 4.30), there is a slight increase in the working fluid in the lower part of the plume for the Model M2 fan.

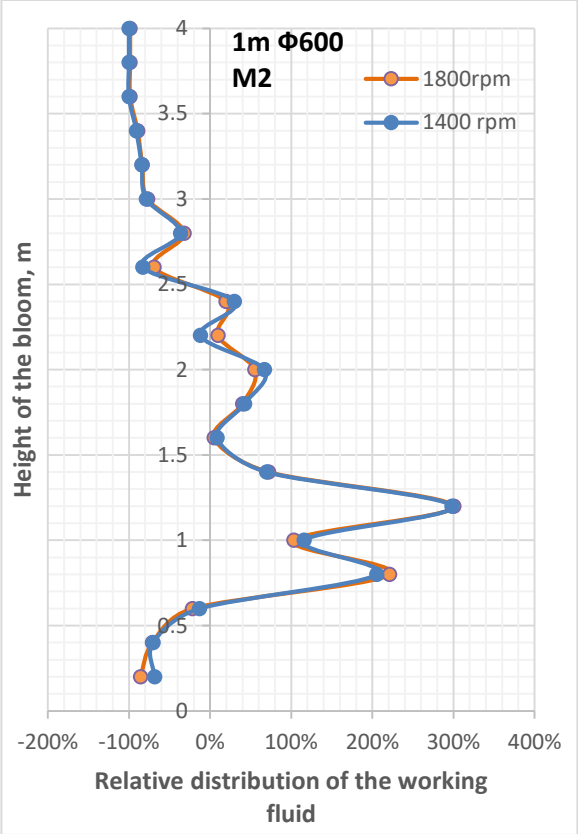


Figure 4.29. Relative distribution of the working fluid at a distance of 1 meter from the 600mm diameter Model M2 fan.

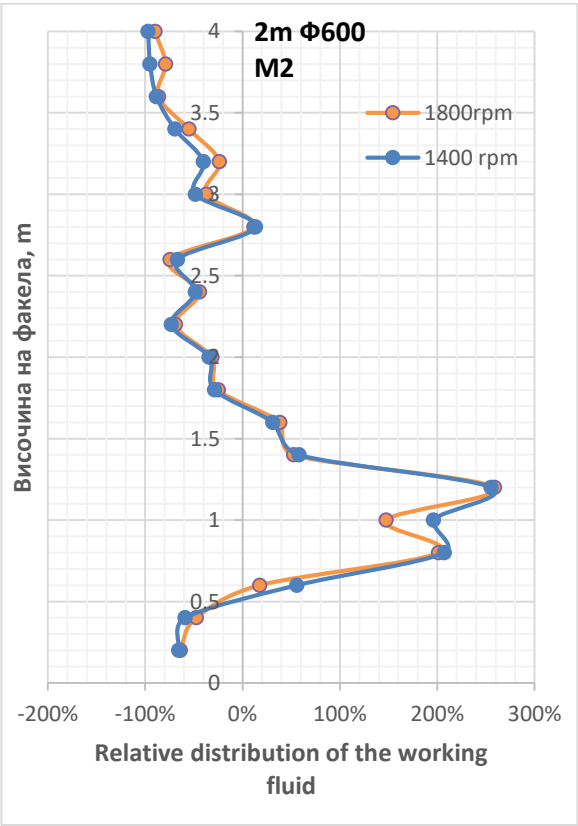


Figure 4.30. Relative distribution of the working fluid at a distance of 2 meters from the 600mm diameter Model M2 fan.

Results from the investigations of the parameters of droplet coverage

When operating the fan-assisted rotary sprayer, working fluid is sprayed simultaneously with the creation of an airflow by the fan. To assess the parameters of droplet coverage, and consequently, the sizes of the generated droplets, droplet imprints are taken using water-sensitive paper. Water-sensitive paper has a specified spreading coefficient. With the program and algorithm described in the Theoretical Studies section, the obtained droplet coverages for the investigated rotary sprayers and operating modes were evaluated. Based on the presented overall appearance of droplet coverage in Figure 4.31, taken in triplicate for each experiment, the parameters of the droplet coverage were determined.

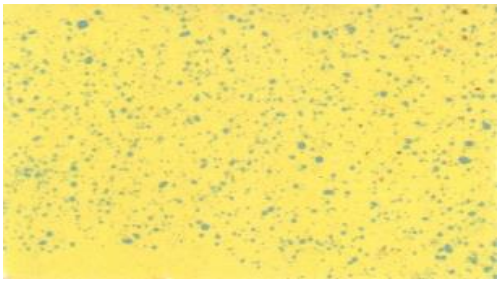


Figure 4.31: General view of droplet coverage.

Results of the investigations of the parameters of droplet coverage for the fan rotational sprayer with a 500 mm diameter

The result of the analysis of the obtained droplet imprints reflecting the relationship between the mean droplet diameter and the rotational speed of the sprayer at different flow rates for the fan rotational sprayer with a 500 mm diameter is shown in Figure 4.32. It can be seen that with an increase in rotational speed, the mean droplet diameter experiences a slight decrease. Practically, there is no influence on the droplet sizes from the different flow rates used. This indicates that within this range of flow rates, the spraying mechanism manages to disperse the supplied liquid without serious overloading or hindrance to its operation.

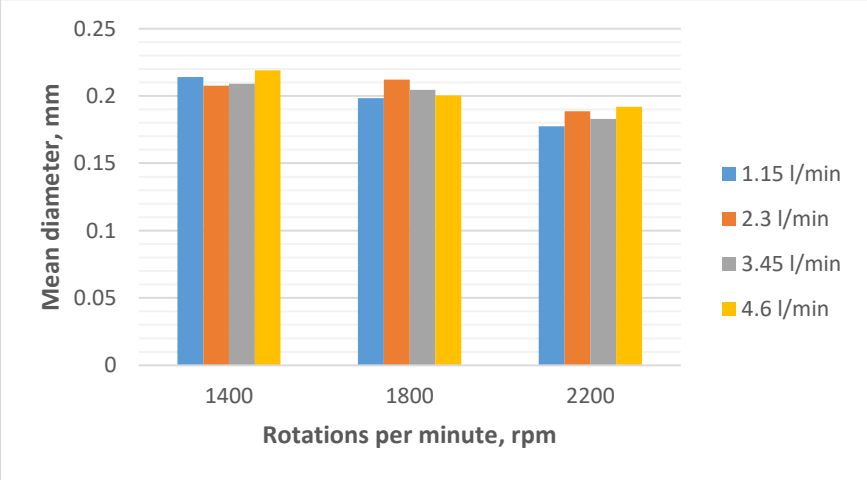
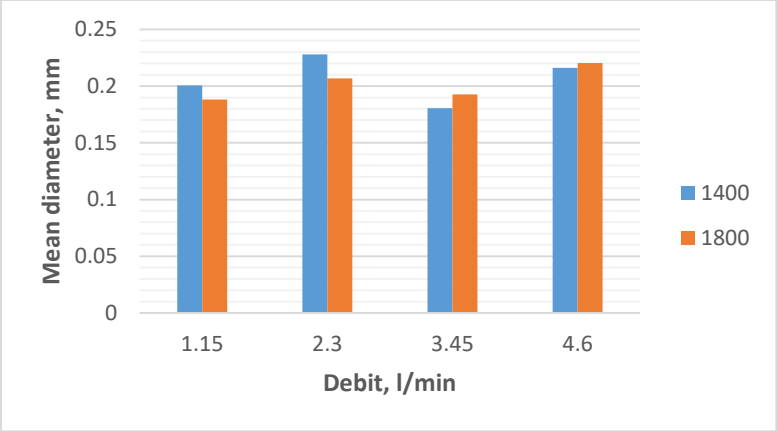


Figure 4.32. Dependence of the mean droplet diameter on the rotational speed of the sprayer at different flow rates of the spraying system.



Results of the studies on the parameters of droplet coverage in the 600 mm diameter fan rotational sprayer with the M1 fan modification

The change in the mean droplet diameter is logically similar in different modes and in the 600 mm diameter fan rotational sprayer with the M1 fan modification, as shown in Figure 4.33. This is because the sprayer is the same and demonstrates that the airflow has relatively little influence on the droplet size. There is a slight increase in diameter with an increase in flow rate, as seen in Figure 4.33.

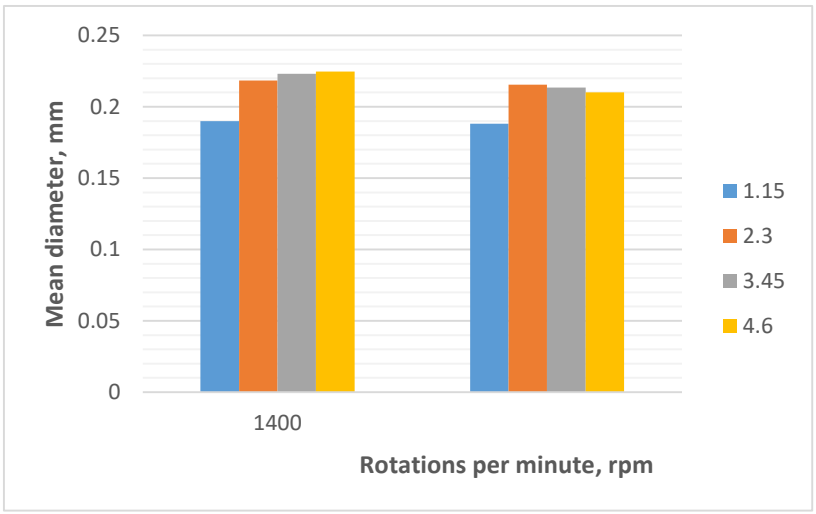


Figure 4.33: Dependency of the mean droplet diameter on the rotational speed of the sprayer at different flow rates of the spraying system.

Results of the investigations on the parameters of droplet coverage in the case of the 600 mm diameter fan and the M2 modification of the fan.

The influence of the operating mode is similar for the 600 mm diameter fan with the M2 modification, as shown in Figure 4.34. For all the fans used with this type of rotary sprayer, the mean droplet diameter is around 0.2 mm.

Figure 4.34. Dependence of the mean droplet diameter on the flow rate of the spraying system at different fan rotation speeds.

Results of the investigations of a potential pump for delivering the working fluid to the fan rotational atomizers

Based on an in-depth market study for pumps suitable for use in the spraying system of this type of fan-like rotary sprayers, we have selected the SINGFLO FL-40 pump model for integration into our sprayer. The pump has the following parameters: Voltage: 9 – 14V; Flow rate: 17 l/min; Cut-off pressure: 2.8 bar adjustable; Current consumption: 9.2A. Description: Two-chamber diaphragm; Inlet and outlet: quick-connect fittings – for 16 mm hose and standard 1/2" thread; Liquid: water up to 60°C; Self-priming: up to 1.5 m elevation difference; 12V electric motor with permanent magnets; Thermal overload protection with automatic restart.

The selected parameters allow the pump to be powered by the tractor's electrical system, and in the event of a blockage in the supply system and an increase in pressure, it will shut off to protect the other components of the system. To establish and confirm the capabilities, a study was conducted on the relationship between the achieved working pressure and the consumed current, as shown in Fig. 4.35. It can be seen that with a current consumption of 9.8A, a working fluid pressure of 2.5 bar can be achieved. Since a pressure of 1 bar is sufficient for this type of spraying system, this implies a consumption not exceeding 9A.

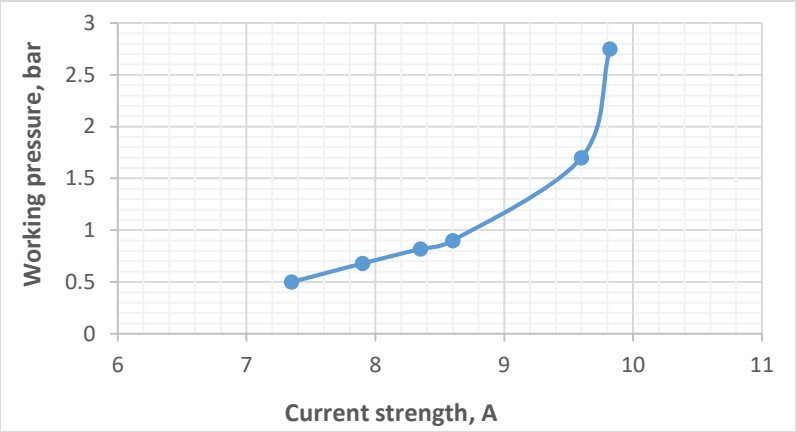


Fig. 4.35. Relationship between the generated working pressure and the strength of the consumed current

From the study of the obtained flow rate, current consumption, and the required voltage, it can be seen that a flow rate of 10-12 l/min, sufficient to meet the requirements for the necessary fluid application rate for treating perennial crops with this type of working equipment, is achieved at the tractor's battery voltage and a current consumption of 6-7A, as shown in Fig. 4.36. These current parameters will not overload the tractor's electrical system, and the sprayer can be equipped with such a pump.

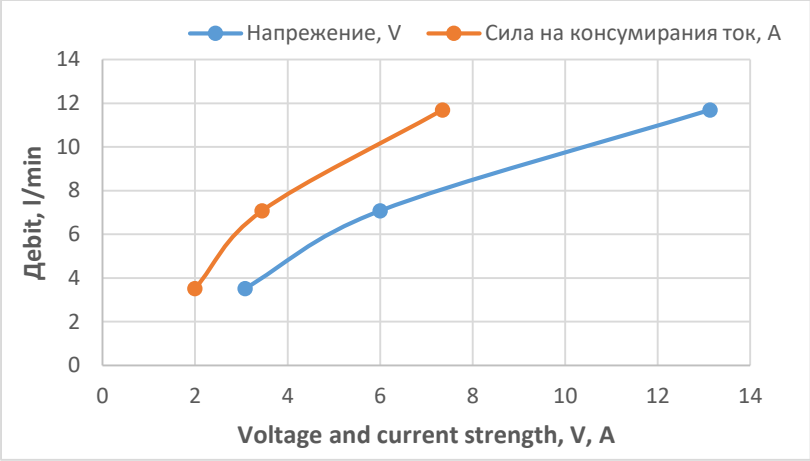


Fig. 4.36. Relationship between the flow rate and the voltage and the strength of the consumed current

Model sample of a sprayer

On Fig. 4.37, the model sample of a sprayer for perennial crops for small-scale farms with fan-like rotary sprayers is shown.

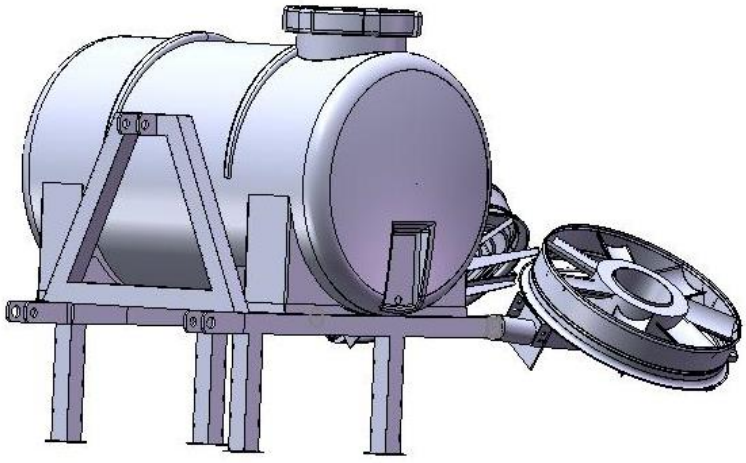


Fig. 4.37. Model sample of a sprayer with fan-like rotary sprayers.

CONCLUSIONS

1. The profile of the airflow obtained from a 500 mm diameter fan at a speed of 1400 rpm initially has a bimodal shape in the vertical direction, which gradually becomes unimodal at a distance of 3 m. At a height of 1.25 m, the airspeed reaches 8 m/s.
2. For the same fan, F500, at a speed of 1800 rpm, the airflow profile is the same as at 1400 rpm - bimodal in the vertical section at the beginning and unimodal in the horizontal section. The airspeed reaches 9 m/s at a height of 1.5 m and 2.25 m.
3. The same airflow characteristics apply to the fan speed of 2200 rpm, as in the previous two speeds. At a distance of 1 m, the peak airflow velocity reaches 12 m/s, decreasing to 5.5 m/s at 3 m.
4. In the horizontal direction, the profile for this fan is unimodal, illustrating the potential for a smooth increase in airflow velocity during the machine's forward movement, thereby ensuring even coverage of the treated object. The maximum velocity at all three modes and distances is achieved at heights of 1.25-1.5 m.
5. The nature of the change in maximum airflow velocity with increasing fan speed using a 600 mm diameter fan (modification M1) is similar to that of a 500 mm diameter fan. The difference lies in the faster decrease in maximum velocity with increasing distance from the fan. This provides conditions for a gradual swirling of the foliage and more uniform spraying.
6. The airflow profile for a 600 mm diameter fan with modification M2 is similar to that of modification M1. However, unlike M1, this modification has two peaks in airflow velocity.
7. The change in average airflow profile velocity for a 500 mm diameter fan varies with the distance from the fan. The smallest decrease in velocity with increasing distance from the fan occurs at a fan speed of 1800 rpm, making this mode preferable for operation with this fan.
8. The average airflow velocities decrease more rapidly with increasing distance when using a 600 mm diameter fan model M1 in both speed modes compared to a 500 mm diameter fan.
9. The average airflow velocities using a 600 mm diameter fan model M2 hardly depend on fan speed and are less affected by distance. This highlights the importance of blade shape on airflow parameters.
10. The relative distribution of the working fluid with a 500 mm diameter fan and five blades is bimodal, with the height of the peaks decreasing with distance from the fan. The upper peak is larger for this fan and relatively decreases with distance. The standard deviation increases from 7% at 1 m distance to 14% at 3 m.
11. The working range of the 500 mm diameter fan extends from 0.8 m to 2.4 m at a 1 m distance, increasing to 3.5 m at 3 m distance.
12. The relative distribution of the working fluid for a 600 mm diameter fan with seven blades is unimodal and less uniform than that of a 500 mm diameter fan. The standard

deviation increases from 6% at 1 m distance to 15% at 3 m for model M1 and from 12% to 16% for model M2.

13. The study shows that the formation of the air jet by the three different spray devices, with varying diameters and numbers of blades, affects the distribution of the working fluid differently. Fan speed has very little influence on relative distribution.
14. The research indicates that by choosing a specific working device that matches the condition of the treated perennial crop, maximum biological and economic efficiency can be achieved. Based on the relative distribution, the use of 600 mm diameter air rotary sprayers is recommended for predominantly vineyard treatments and 500 mm diameter sprayers for fruit orchards.
15. The average droplet diameter of the spray does not depend on the parameters of the airflow generated by the fan.
16. The chosen pump type (SINGFLO FL-40) for powering this spraying system meets the requirements for providing the necessary flow rate and pressure. The current consumption at these requirements will not burden the tractor's electrical system.

CONTRIBUTIONS

1. Preconditions have been defined for increasing the effective utilization of pesticide formulations, improving eco-economic efficiency, and reducing losses.
2. A coefficient of useful pesticide utilization has been justified, allowing for a quantitative assessment of pesticide use by purpose.
3. A graphical interpretation has been proposed that can be used for planning the consumption rate depending on the recommended density, droplet diameter, and plant development for specific activities.
4. An algorithm and program have been developed for assessing the parameters of droplet prints, allowing for the determination of the key indicators for evaluating the quality of droplet coverage regardless of the carrier of the print.
5. The airflow profile has been determined, along with its dependence on the structural parameters of the fan shaft.
6. The distribution of the working fluid by height and the factors influencing it have been identified for the studied fan-like rotary sprayers.
7. The results confirm the hypothesis of a possible choice of a working device tailored to the formation and condition of the treated perennial crop to achieve maximum biological and economic efficiency.
8. It has been established that the average droplet diameter in the studied fan-like rotary sprayers is not influenced by the parameters of the airflow.
9. The elements of a fan-like rotary spraying system for perennial crops designed for small farmers have been justified, creating conditions for achieving maximum biological and economic efficiency in treating perennial crops.
10.

PUBLICATIONS RELATED TO THE DISSERTATION

1. Blagoj Elenov, Ivan Mortev, Elena Dimitrova, (2019) - "Features of Mechanizing Plant Protection Measures," International Scientific Conference "Conserving Soils and Water 2019," Burgas, 3, (1), 2019, pp: 117-121 ISSN (PRINT) 2535-0234, ISSN (ONLINE) 2535-0242. (In BG)
2. Blagoj Elenov (2020) - "Sprayers for Perennial Crop Protection," Proceedings of the International Scientific Conference for Young Scientists "Management and Quality,", Sofia, June 2020. pp: 13- 18 ISSN (PRINT) 2603-4395 (In BG)
3. Blagoj Elenov, Georgi Kostadinov, "Influence of Technical and Technological Parameters of an Air Rotary Sprayer Fan on the Distribution of Working Fluid in the Treatment of Perennial Crops," Plant Sciences, 5, 2023 (in print). ISSN 0568-465X (Print) ISSN 2534-9848 (Online) (In BG)

ACKNOWLEDGEMENTS

I express my gratitude to my academic supervisor, the management of the Institute of Agricultural Engineering (ISSAPP) 'Nikola Pushkarov,' and my colleagues from the 'Agricultural Machinery and Hydraulic Reclamation Systems' section for the material and practical assistance provided in conducting the experiments and shaping this dissertation work.